

OFFICIAL DOCUMENT

DO NOT REMOVE FROM
THE RESEARCH OFFICE

FATIGUE CRACKING IN MODULAR EXPANSION JOINTS

WA-RD 306.1

Final Report
June 1993



**Washington State
Department of Transportation**

Washington State Transportation Commission
Transit, Research, and Intermodal Planning (TRIP) Division
in cooperation with the U.S. Department of Transportation
Federal Highway Administration

TECHNICAL REPORT STANDARD TITLE PAGE

1. REPORT NO. WA-RD 306.1	2. GOVERNMENT ACCESSION NO.	3. RECIPIENT'S CATALOG NO.	
4. TITLE AND SUBTITLE FATIGUE CRACKING IN MODULAR EXPANSION JOINTS		5. REPORT DATE June 1993	
7. AUTHOR(S) Charles W. Roeder		6. PERFORMING ORGANIZATION CODE	
9. PERFORMING ORGANIZATION NAME AND ADDRESS Washington State Transportation Center (TRAC) University of Washington, JE-10 The Corbet Building, Suite 204; 4507 University Way N.E. Seattle, Washington 98105		8. PERFORMING ORGANIZATION REPORT NO.	
12. SPONSORING AGENCY NAME AND ADDRESS Washington State Department of Transportation Transportation Building, MS 7370 Olympia, Washington 98504-7370		10. WORK UNIT NO.	
13. SUPPLEMENTARY NOTES This study was conducted in cooperation with the U.S. Department of Transportation, Federal Highway Administration.		11. CONTRACT OR GRANT NO. T9233, Task 33	
16. ABSTRACT <p> Modular expansion joints are commonly used on bridges with potential movements larger than approximately 5 inches. Single support bar modular systems with 48 inches of movement capability were used for the third Lake Washington Floating Bridge. Within 18 months after the bridge was opened to traffic, cracks were noted in the centerbeams of these large, modular systems. Additional cracks have occurred. </p> <p> This research program was a study into the causes of the observed cracking. The work was divided into two tasks. The first task was a literature review and evaluation of existing methods for fatigue design of modular joint systems. The second task consisted of a wide range of finite element analyses of the particular joint, and correlation of the computed results in existing design models and observed behavior. </p> <p> The results show that the cracking has been caused by fatigue due to repeated wheel loading. However, existing design methods do not appear to be reliable indicators of the fatigue behavior because the behavior is influenced by the stiffness and dynamic response of the individual joint system. The variable span lengths complicate the evaluation process. The work shows that there is no reliable information for the wheel load spectrum for U.S. traffic on joints of this type. However, extension of past behavior of this joint indicates that centerbeams of the large joint will require replacement before its expected design life of 25 to 30 years has been achieved. </p>		13. TYPE OF REPORT AND PERIOD COVERED Final report	
17. KEY WORDS Cracking, expansion joints, fatigue, modular expansion joints, steel		14. SPONSORING AGENCY CODE	
19. SECURITY CLASSIF. (of this report) <p style="text-align: center;">None</p>		18. DISTRIBUTION STATEMENT No restrictions. This document is available to the public through the National Technical Information Service, Springfield, VA 22616	
20. SECURITY CLASSIF. (of this page) <p style="text-align: center;">None</p>		21. NO. OF PAGES <p style="text-align: center;">52</p>	22. PRICE

Final Report
Research Project T9233, Task 33
Preliminary Investigation of Fatigue Cracking in Modular Expansion Joints

**FATIGUE CRACKING IN
MODULAR EXPANSION JOINTS**

by

Charles W. Roeder
Department of Civil Engineering, FX-10
University of Washington
Seattle, Washington 98195

Washington State Transportation Center (TRAC)
University of Washington, JD-10
University District Building
1107 NE 45th Street, Suite 535
Seattle, Washington 98105-4631

Washington State Department of Transportation
Technical Monitor
John Van Lund
Bridges and Structures Office

Prepared for

Washington State Transportation Commission
Department of Transportation
and in cooperation with
U.S. Department of Transportation
Federal Highway Administration

June 1993

DISCLAIMER

The contents of this report reflect the views of the authors, who are responsible for the facts and the accuracy of the data presented herein. The contents do not necessarily reflect the official views or policies of the Washington State Transportation Commission, Department of Transportation, or the Federal Highway Administration. This report does not constitute a standard, specification, or regulation.

TABLE OF CONTENTS

<u>Section</u>	<u>Page</u>
Summary	1
Conclusions and Recommendations	2
Conclusions and Observations	2
Recommendations	5
Introduction	7
Research Objectives	7
The Problem	7
Review of Previous Work	10
Procedures	14
Task 1 — Evaluation of the Tschemmerneegg Method	14
Task 2 — Analysis of the Modular Joint System.....	15
Static Global Finite Element Analysis	16
Static Local Finite Element Analysis	19
Dynamic Analyses.....	20
Discussion	26
Combination of Static and Dynamic Response.....	26
Horizontal Component of Force.....	28
Correlation of Computed Stress to Fatigue Criteria.....	28
Other Issues	34
Lake Level and Seasonal Effects	34
Effect of Tubular Center Beams.....	35
Residual Stress	35
Fatigue Cracking in Other Center Beams	36
Effect of Smaller Joint Size.....	39
Replacement Center Beams	39
Variations in Wheel Loads and Geometry	40
References	52

LIST OF FIGURES

Figure		Page
1.	Photo of a Crack in a Center Beam at the Toe of the Stirrup Weld..	9
2.	Photo of a Crack at an Earlier Repair.....	9
3.	S-N Curve Proposed for the Tubular Center Beams.....	13
4.	Construction Method for the S-N Curve.....	13
5.	Finite Element Model of Entire Modular Expansion Joint LM Line Pontoon A1 or R1 Eastbound.....	22
6.	Model of Typical Center Beam.....	22
7.	Typical Load Placement on Modular Expansion Joint LM Line Pontoon A1 or R1 Eastbound.....	23
8.	Bending Moment Diagram for a Center Beam at the Edge of the Joint and with Truck Wheels in the Outside Lane.....	23
9.	Moment Diagram for the Center Beam of Figure 8 with Wheel Loads in the Adjacent Lane of Traffic.....	24
10.	Local Finite Element Model.....	24
11.	Local Deformation of the Stirrup and Center Beam.....	25
12.	Typical Vertical Modes of Vibration.....	25
13.	Idealized Dynamic Loading on a Center Beam.....	47
14.	Dynamic Amplification for a Ramp Function Loading.....	47
15.	Present AASHTO S-N Curves for Categories D and E.....	48
16.	Photo of Fatigue Cracking from Tschemmernegg Failure Test.....	48
17.	AASHTO LRFD S-N Curves Compared to a Range of Different Tschemmernegg S-N Curves.....	49
18.	Bending Moment Diagram for a Middle Center Beam CB7 with Truck Wheels in the Outside Lane (LP2).....	49
19.	Moment Diagram for CB7 with Wheel Loads in the Adjacent Lane of Traffic (LP3).....	50
20.	Approximate S-N Curve Translated to a Time Scale.....	50
21.	Geometry of Proposed Replacement Center Beams.....	51
22.	Geometry Used for Distributed Wheel Load.....	51

LIST OF TABLES

Table		Page
1.	Stress Range Levels for Location A of CB13	43
2.	Stress Range Levels for Other Center Beams and Locations.....	44
3.	Stress Range Levels for Other Joint Systems.....	45
4.	Stresses for Concentrated and Distributed Wheel Loads on CB13...	46

SUMMARY

This report describes an analytical study of cracking observed in the large modular expansion joints on the third Lake Washington Bridge. Because of uncertainties about the loading and load spectrum on these joints, the interpretation of the computed results is imprecise. However, a number of important observations can be made.

CONCLUSIONS AND RECOMMENDATIONS

CONCLUSIONS AND OBSERVATIONS

The researchers are reasonably certain that the cracking is a result of fatigue caused by cyclic loads induced by wheel loads on the joint. The precise cause of the fatigue problem cannot be determined, but a number of factors that affect the fatigue have been isolated. These include the following.

1. The fatigue problem is most serious and pressing in the edge girders of the large expansion joint because of the larger stress and stress range produced by the variable spans in the edge girders of the single support bar system.
2. Large bending stresses are introduced by truck wheel loads on the modular joints. The stresses are often in compression, but residual stresses near the stirrup-to-center-beam weld may cause the entire cyclic compressive stress to be in cyclic tension.
3. The tubular center beams clearly contribute to the fatigue problem because they cause local deformation and through-thickness plate bending stress. The actual extent of this effect is difficult to quantify because of the lack of a reliable S-N curve for combined cyclic bending and local deformation. Despite the local deformation, fatigue would almost certainly have been a problem even if another section had been used for the center beams.
4. The Tschemmernegg fatigue test on a tubular center beam is not indicative of the fatigue behavior of this joint because it does not develop the crack pattern and failure mode observed on the joint. The test does not reflect the flexibility of the joint with respect to horizontal loads.
5. Wheel loads cause multiple stress cycles for a single truck passage, and thus the fatigue evaluation procedure of modular expansion joints must be

somewhat different than that for bridge girders and other structural elements. The analysis showed that a much larger stress range is possible between individual trucks because the trucks do not follow the same path across the joint. This variability may double the stress range over that noted for a single wheel load. The stress range due to this variability exceeds the design range used by Tschemmerneegg.

6. The large horizontal forces commonly required by the Tschemmerneegg design procedure may not be appropriate for this particular joint system because of its flexibility. On the other hand, the stiffness characteristics of this particular joint suggest that it may experience greater amplification of gravity loads.
7. The elastomeric bearings, which serve as springs in the modular joint system, have frequently been reported as being loose in the joints, and they are an important element in the joint behavior. The precompression or looseness of the bearings may affect local bending stress in the critical region surrounding the stirrup. The loose bearings may also lengthen periods of critical modes of center beam vibration. However, the loose elastomeric bearings are not thought to be a predominant contributor to the fatigue problems noted in the joints.
8. The Tschemmerneegg design procedure may not be applicable to all modular joint systems because it is based on field measurements, analysis, and fatigue tests of stiff modular joint systems. Modular joints vary greatly from manufacturer to manufacturer and from system to system. Fatigue design criteria for modular joints clearly must consider the unique features and dynamic response of each joint system. The fatigue test must be appropriate for the loads the joint experiences, or it will lead to improper S-N curves and improper modes of failure.

9. The finite element analysis of the smaller modular expansion joint suggest that cracking comparable to that presently seen on the larger expansion joint should appear after 8 years. No cracking of these smaller joints has been clearly identified yet, but the joint is difficult to inspect.
10. A global analysis was performed with the proposed replacement center beams. The proposed replacement beams should eliminate many of the local bending effects in the center beams, but the global bending stresses in the center beams are nearly identical to those predicted with the existing beams. As a result, it is unlikely that the replacement center beam will prevent all future fatigue problems with the DS1200 joint. The fatigue life is likely to be longer with the replacement center beams, but it is difficult to predict the actual increase in service life.
11. The effects of distributed wheel loads and WSDOT legal wheel limits were examined. Distributed loading results in stresses and stress ranges that are approximately 85 percent of those noted with comparable concentrated loads. When the 13-kip (57.9-kN) legal wheel load is used, the stresses are reduced to approximately 81 percent of those noted with a 16-kip (71.2-kN) wheel loading.
12. The behavior of the modular expansion joint is strongly influenced by the dynamic response of the modular joint system. The dynamic response is complicated because hundreds of modes of vibrations may contribute to the response, and so theoretical predictions are approximate. However, these predictions suggest that the response is very sensitive to the type of joint under consideration and the type of loading. This particular modular joint amplifies horizontal loads that are applied slowly, but it amplifies vertical loads through a wide range of vehicle speeds.

13. Analysis suggests that the fatigue damage on this particular expansion joint accumulates more rapidly in the early fall (October) because the joint is more open and has a greater slope at that time, and the traffic is often slower. These factors lead to greater concentration of load on individual center beams and a greater effect of horizontal loads.

RECOMMENDATIONS

With the observations noted above, it is logical to recommend that the center beams in the larger modular joint system be replaced in the next several years. However, the design and selection of a replacement beam will not be a clear and easy choice until better information is available on the load spectrum and amplification characteristics for the joint. Simple replacement of the tubular section with a rail section may not be effective because of the large stress ranges computed and the larger amplification predicted for gravity loads with this modular system. Further, the Tschemmernegg method is unlikely to be an accurate predictor of the fatigue life of these components.

Recommendations for the smaller DS480 expansion joints are less clear. The best estimates performed with analysis to date indicate that they are less susceptible to fatigue. Cracking comparable to that noted in the larger joint is expected after approximately the first 8 years. This suggests that they will require replacement after approximately 10 to 15 years. Better load and/or fatigue life estimates may modify this estimate.

Greater certainty in these observations could be achieved with additional information. The additional information includes the following.

1. The load spectrum and accumulated damage estimates for fatigue life are presently based upon limited field measurements of modular joints. The joint used for these measurements appears to be quite stiff in comparison to joints such as those on the Lake Washington Bridge. Therefore, the load spectrum is of questionable validity. There is further question that truck wheel loads from Europe are applicable to U.S. practice because of

the wide variation of legal truck loads in the U.S. These data are essential for reliable fatigue estimates of these and other modular joints. Accurate fatigue evaluations of this joint or any replacement joint or joint component cannot be made until this information is available. Thus field measurements of the load spectrum and stress range are recommended.

2. Field measurements of the dynamic response of modular joints also would be useful. Damping is likely to be very important, and there is no rational way of estimating damping for the modular joint system without measuring the dynamic response. Further, the dynamic response is complex, and field measurements of dynamic response would assist in evaluating the dynamic response predictions.

INTRODUCTION

RESEARCH OBJECTIVES

The primary objective of this project was to evaluate the cracking problems noted on the modular expansion joints on the third Lake Washington Bridge. Two major tasks were performed as part of this evaluation. These tasks were as follows:

1. provide a peer review of the Patis and Tschemmernegg fatigue evaluation method and proposed repair methods; and
2. complete a detailed computer analysis of the modular system to determine the probable causes of the cracking, further evaluate the proposed repairs, and make recommendations.

THE PROBLEM

The Washington State Department of Transportation (WSDOT) commonly uses modular expansion joints on bridges whose expected movements are larger than 5 inches. Modular joints with a total movement capacity of 48 inches were manufactured by The D.S. Brown Company under license of the Maurer Sohne Company of Munich, Germany, and were installed on the third Lake Washington Floating Bridge. These expansion joints, first subjected to traffic in 1989, are believed to be the largest modular expansion joints in the world. The design is a fairly standard, single support bar system, except that tubes with an extruded rail cap were substituted for the heavy center beams because of Buy American requirements for federally funded bridge construction.

Approximately 6 months after the bridge was opened to traffic, WSDOT received numerous complaints because the expansion joints were noisy. Inspection of the joints showed that the elastomeric bearings used to cushion the traffic impact between the center beams, stirrups, and support bars were loose. Shims were added, but within a year cracks in the center beams were noted. Most of these cracks started at the toe of the

stirrup fillet weld and progressed through the center beam, as shown in Figure 1, but one crack occurred at the end of a reinforcing bar. D.S. Brown repaired seven of these cracks in April 1991 by rewelding the cracked metal. Additional cracks were noted in the center beams after this first repair, and seven more cracks were repaired in November 1991. Additional cracks were noted after this second repair, and some of the previously repaired cracks reappeared, as shown in Figure 2.

WSDOT had a number of concerns regarding the observed cracking. WSDOT was concerned that the cause might be related to a fundamental flaw in the modular joint system or that the problem might be related to the substitution of the tubular section to be used as the center beams for the heavy rail sections used in the original Maurer design. WSDOT was concerned about the elastomeric pads and the fact that they were loose under some conditions, and the many special conditions of the third Lake Washington Floating Bridge, including heavy traffic, a sloped traffic lane, changing lake levels, long expansion distance, and other factors. This research project was initiated to address these concerns and provide recommendations for alleviating them.

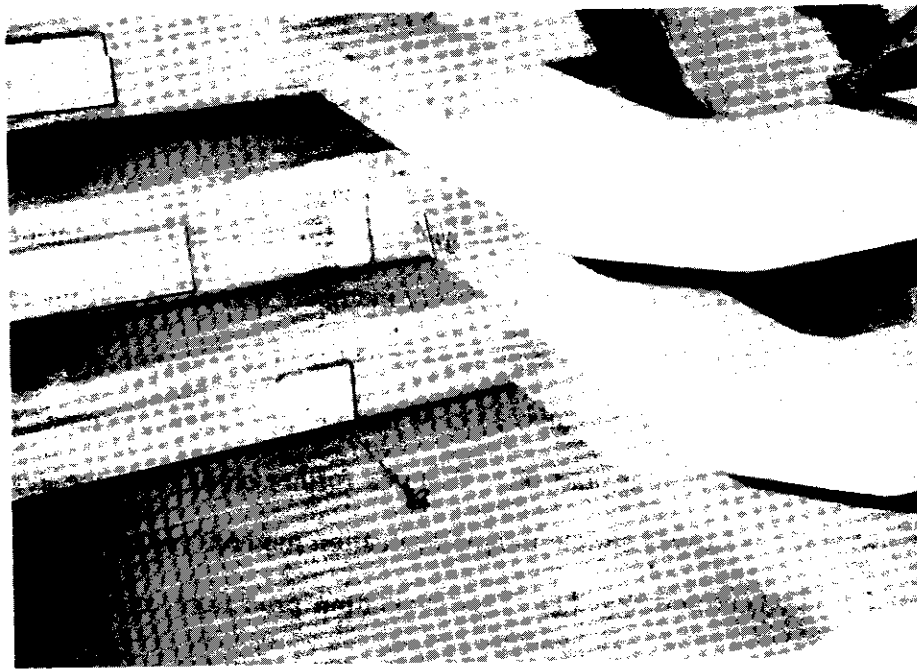


Figure 1. Photo of a Crack in a Center Beam at the Toe of the Stirrup Weld



Figure 2. Photo of a Crack at an Earlier Repair

REVIEW OF PREVIOUS WORK

There has been very little study into the fatigue life of modular expansion joints. These joints are quite complex. They have many members that move and interact with one another, and this complicates the evaluation of the load distribution and movement capabilities. In addition, each modular system has unique (often patented) features contributed by the manufacturer, and these features further complicate the evaluation process. However, a relatively simple fatigue evaluation method has been proposed by A. Patts and F. Tschemmernegg. [1] This evaluation procedure relies on a simply calculated stress, which is compared to the endurance limit from the S-N curve obtained from fatigue test results. The calculation is based on the assumption of rigid support behavior.

The Patts and Tschemmernegg fatigue evaluation method [1, 2] is a relatively simple, four-step procedure, which is used by some bearing manufacturers. [3] First, the loads on the bridge and the expansion joint are determined. These loads include a vertical component attributable to gravity load and a horizontal component attributable to traffic acceleration, braking, and rebound forces. The recommended wheel loads, including impact, are vertical loads of a maximum of +20,000 lbs (+89 kN) and minimum of -6,000 lbs (-26.7 kN), and a horizontal force of $\pm 4,000$ lbs (± 17.8 kN). The full spectrum of truck wheel loads are considered. The design spectrum and the magnitudes of the horizontal and uplift loads are based on field measurements from bridges in Europe. [4] With this spectrum, the maximum load is expected only in approximately 10,000 of each 200 million cycles.

Second, the stresses in the center beams and support bars are calculated to determine the maximum computed stress range, $\Delta\sigma_{\max}$. The center beams are treated as continuous beams, and the elastic parts of the expansion device are treated as rigid supports for determination of the moments and the stress level. For normal conditions,

each center beam is assumed to carry 50 to 60 percent of the wheel load with the wheel spacing at 6 ft, since the wheel distributes the load to more than one center beam. Note that the primary loading considered in the design method produces compressive stress in the same area as the fatigue cracking on the third Lake Washington Bridge. Fatigue design practice has historically focused on the total stress range, and mean stress is ignored. [5]

Third, this maximum stress range is compared to an S-N curve developed from experimental results. The comparison considers the full load spectrum and the accumulation of damage attributable to variable amplitude loading through the combination of Miner's rule and the load spectrum. [4] These factors are accounted for by the partial safety factor, γ_{MF} and α , where α accounts for accumulated fatigue damage by Miner's rule.

Separate S-N curves are provided for the center beams, the support bars, and the connection between them. Figure 3 shows an S-N curve that has been proposed for the tubular center beams used in the third Lake Washington Floating Bridge. [6] The endurance limit, $\Delta\sigma_L$, is intended to be the stress level that can develop 100 million cycles of loading, but it is inferred from an interpretation of experiments performed at stress ranges with fatigue lives of less than 2 million cycles. The slope of the log-log S-N curve is assumed to be -0.33 for a stress range of less than 5 million cycles and -0.2 for a stress range between 5 million and 100 million cycles, as illustrated in Figure 4. The intercept at 100 million cycles is accepted as the endurance limit.

Fourth, the design comparison is then

$$\frac{\Delta\sigma_{\max}}{2} < \Delta\sigma_L . \quad (\text{Eq. 1})$$

where $\Delta\sigma_{\max}$ is the calculated stress range based on the defined range of wheel loads, and $\Delta\sigma_L$ is the limit states fatigue stress range (fatigue or endurance limit) at 100 million

cycles, as determined from the fatigue tests. The maximum stress range is divided by 2 because of the accumulated damage rule and the partial safety factor.

The Tschemmerneegg design procedure is the only complete procedure for fatigue design of modular expansion joints. However, there are reasons for questioning the validity of the procedure. Koster suggests that the rigid assumption used in the Tschemmerneegg method is inappropriate. [7] Koster believes that the elastic deformation of the system affects the stress distribution and the fatigue potential. The Tschemmerneegg method is based on test results performed with idealized load and boundary conditions with rigid supports. The calculated design moments and stress ranges may consider some of the flexibility in the components, but the method is predominantly based on rigid supports and connections. Koster contends that deformability of the joint is desirable because it may spread the load and possibly reduce the critical fatigue stress. This latter position is logical, but the elastic deformation and stress distribution are very complicated in a modular joint system.

Agarwal performed a series of field measurements on a modular expansion joint on a bridge in Ontario, Canada. [8] These field measurements suggested that the loads and load spectrum used in the Tschemmerneegg procedure are not universally applicable. They did not detect the large horizontal forces noted by Tschemmerneegg [4], and the load range and spectrum were different. However, the instrumentation that Agarwal used may not have been adequately sensitive to detect the true horizontal loads on the joint.

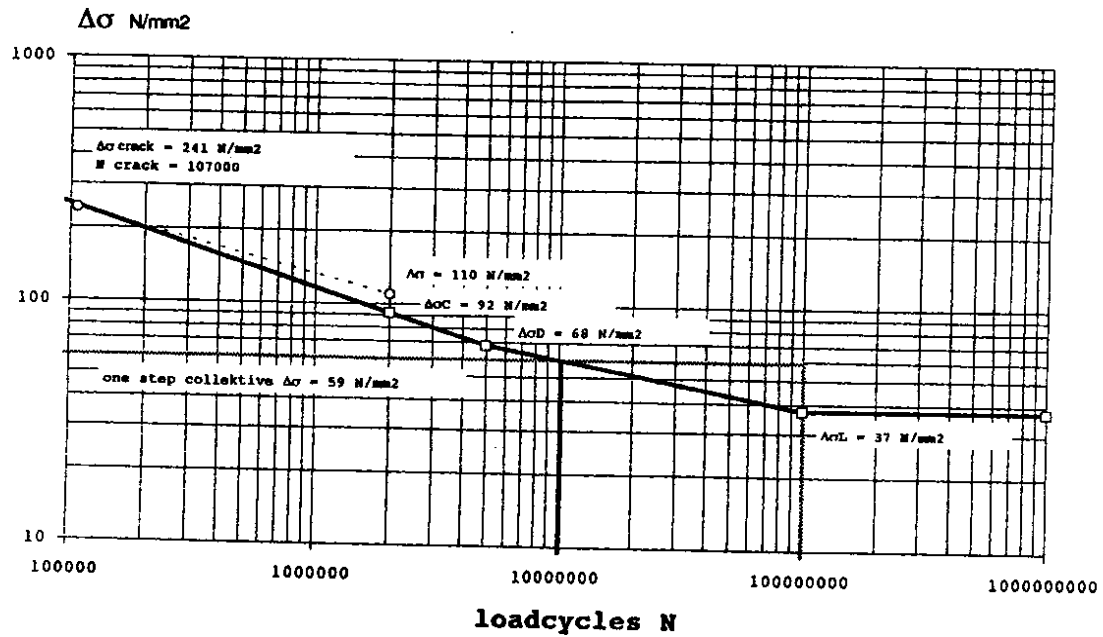


Figure 3. S-N Curve Proposed for the Tubular Center Beams

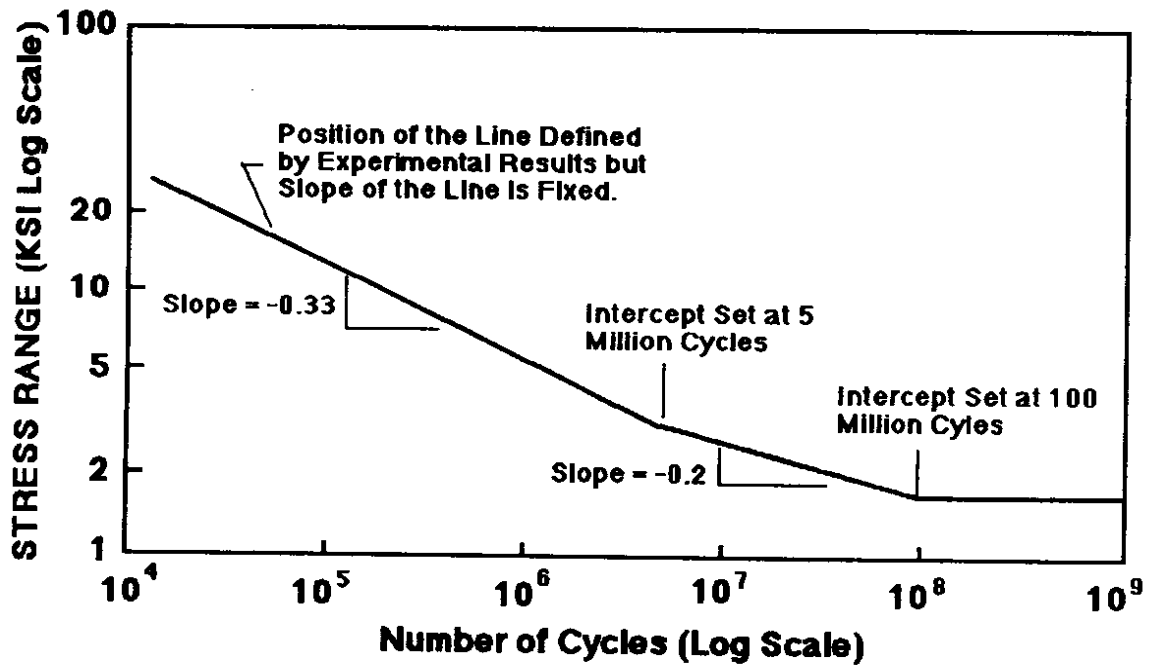


Figure 4. Construction Method for the S-N Curve

PROCEDURES

The research was divided into two major tasks. The first task consisted of a thorough review and evaluation of the Tschemmernegg design method and other related methods. The second task consisted of a detailed analysis of the modular joints on the third Lake Washington Floating Bridge.

TASK 1 — EVALUATION OF THE TSCHEMMERNEGG METHOD

The literature review and evaluation of the Tschemmernegg fatigue design method was completed in the first two months of the research and was summarized in a preliminary report. [9] The method and documents behind the design procedure were read and evaluated in detail, and they were compared to other standard fatigue evaluation procedures. The evaluation raised several important questions about the method. These include the following.

1. There is reason to question the validity of using European wheel loads and load spectra to simulate U.S. traffic. European wheel load ratings are similar to those used in the U.S., but the expansion joint load spectrum also depends on vehicle overloads and the dynamic characteristics of the vehicle and the expansion joint. Agarwal's experiments suggest that they are not applicable to a specific bridge in Canada, and the load and spectrum assumptions have a great influence upon the accumulated damage estimate.
2. The fatigue limit and S-N curve were developed from sparse and distant test results. The design method makes use of the predicted stress range for 5 million to 100 million cycles, but all the test results are performed for less than 2 million cycles. Therefore, it is logical to question the accuracy of the method and fatigue life estimates.

3. The method neglects the effect of elastic deformation of the elastomeric bearings and support beams on the center beams.
4. Photos of fatigue cracking obtained during a test of a tubular center beam showed a different pattern of cracking than was observed on the subject joint. [7] The fatigue tests also produce longitudinal cracks that were not noted at any location on the Lake Washington Bridge. In addition, the transverse-through-depth cracking noted in the field are not obtained in the tests. These observations raise further concerns regarding the applicability of the testing and evaluation procedure to these particular joints.
5. The fatigue tests used in the Tschemmernegg method create primarily compressive bending stress in the cracked region of the center beam. Standard practice in fatigue design neglects mean stress, and thus the total stress range is the element of major concern. However, experts agree that mean stress has some affect on fatigue life. [5] This is sometimes noted by the K factor, where

$$K = 1 - \frac{\sigma_{\min}}{\sigma_{\max}} \quad (\text{Eq. 2})$$

This equation leads to a K value of 2.0 for the zero mean stress condition. Many of the Tschemmernegg tests were performed with a K value of between 0.92 and 0.96 in the compressive range. A K value of 0.96 would not be unusual if the entire stress range were in tension. However, the use of this K value with the entire stress range in nominal compression is questionable.

TASK 2 — ANALYSIS OF THE MODULAR JOINT SYSTEM

The modular joints used in the third Lake Washington Bridge were analyzed in detail to further address questions and issues raised in the first task of the research. The

DS1200 modular joint at the west end of the eastbound lane was analyzed with the SAP90 finite element analysis computer program. [10] The joint was analyzed as a global model, and the results of the global analysis were used to evaluate local effects near fatigue cracking. These initial analyses were static analyses that did not include any dynamic response or impact.

Static Global Finite Element Analysis

The entire joint was analyzed with the center beams, support bars, and stirrups modeled as beam elements in the joint's nominal geometry. The geometry and member properties and stiffness were based on information obtained from the contract shop drawings. The elastomeric pads were modeled as compression and shear springs, where the spring stiffness was determined by typical models of elastomeric bearing stiffness. [11] The shop drawings were not specific regarding the stiffness of these elastomeric springs, and so a parameter study was performed to determine the sensitivity of the computed response to the elastomer stiffness. Only modest variations in bending moments, deflections, and deformations were noted when the spring stiffness was doubled and divided by two; therefore, the possible variations in the elastomeric spring stiffness were not regarded as important. While the elastomeric spring stiffness did not have a dramatic effect on the bending moments, it did have a significant effect on other issues, as will be noted later in the report. Further, the behavior noted with elastomeric springs was quite different from that noted when rigid connections between the support bars and center beams were employed.

A large number of joints and members were required for these analyses, and Figure 5 depicts the overall model of the joint. Figure 6 shows a more detailed picture of the joints and members required to model a center beam and its stirrups. The initial analyses were performed with a standard, vertical, 16-kip (71.2-kN) wheel load with a 6-feet (1.83-m) wheel spacing. No horizontal load was applied during this initial analysis. The static load was distributed to several support beams in the ratio of 25

percent, 50 percent, and 25 percent. This distribution followed the distribution method Tschemmernegg suggested using when the joint is in its intermediate open position. [2] Tschemmernegg suggested that the distribution of wheel load to center beams depends upon the width and spacing of the center beams, and that the middle center beam receives a larger portion of the load at the nominal or expanded geometry and a smaller portion of the load if the joint is compressed. Figure 7 illustrates a typical load placement on the modular expansion joint.

Bending moment diagrams were computed for the various center beams, with vehicle wheel loads at different load positions on the joint. Four load positions (or truck travel paths) were used over one half the bridge. Only one half the bridge required analysis because the joint is nearly symmetric about the center line. This variation simulated trucks in the various lanes of traffic, as well as in different positions on the joint. It produced the full variation in stress states expected with traffic loading. Figure 7 shows the loading distribution for load position LP2 centered over center beam CB13. Figure 8 shows the moment diagram of an edge center beam (CB13) and its stirrups. The figure shows that the bending moment in the center beam was large near the stirrup weld. This moment diagram produced tensile bending stress at the stirrup weld at critical location A and compressive bending stress at the weld of critical location B. Figure 9 shows the same center beam with the wheel loads simulating a truck in the adjacent lane position (LP3). The bending moment with this load position produced a sign reversal for the bending moment and stress at all three critical locations. The normal AASHTO fatigue design procedure uses the stress range defined by the maximum stress that results from the HS-20 truck loading. [12] However, a comparison of Figures 8 and 9 shows that a larger stress range may have been achieved because of wheels placed on adjacent traffic lanes. Further, AASHTO regards 2 million repetitions of the AASHTO truck loadings as an appropriate number of design load cycles, but this analysis suggests that

the number of cycles depends upon the number of axles crossing the joint and that it may be exacerbated by trucks passing in adjacent lanes.

Bending moment diagrams were also obtained for other center beams. Similar behavior was noted for other center beams, but the bending moments and nominal stress ranges were smaller when the load was placed on interior center beams than on edge center beams. The researchers determined that the reason for this observation was that spans for the edge center beams were variable with the single support bar modular joint system, but the interior center beams had more uniform span lengths. The more uniform spans appeared to reduce the range of the stress and the bending moments at the critical stirrup locations. This result suggests that the center beams near the edge of the modular joint are more likely to experience early fatigue cracking than the interior members.

Global analyses were also performed with horizontal loads applied to the joint. Torsional deformation of the center beams resulted when these horizontal loads were applied at the top of the center beam rail. The bending moments caused by lateral loads and the resulting bending stresses were all computed. Horizontal loads of 5 percent, 10 percent, 20 percent, 30 percent and 40 percent of the nominal 16-kip (71.2-kN) wheel load were applied, and they were distributed to the center beams by the same proportions used for the gravity load. The system was surprisingly stiff against these horizontal loads because horizontal deflections of the center beam were no more than approximately 0.35 inch (8.9 mm), even with the largest horizontal loads. The bending stresses in the center beams near the critical stirrup locations were also noted. The minor axis bending stress at the critical stirrup location was in the order of 0.25 ksi (1.7 MPa) when the lateral wheel load was 5 percent of the 16-kip (71.2-kN) gravity load and approximately 2 ksi (13.8 MPa) with a 40 percent horizontal loading. Complete reversals were noted when the truck wheels were placed in alternate positions, as noted earlier in the gravity load analysis. Thus, the potential stress range in the center beam at the stirrups were in the order of 0.5 ksi (3.45 MPa) and 4.0 ksi (27.6 MPa) with horizontal truck wheel loads

in the order of 5 percent and 40 percent of the 16-kip vertical wheel loading, respectively. Note that the bending moments and bending stresses for both weak axis and strong axis bending were much larger at locations other than the stirrup connection. The maximum bending moments and bending stresses were sometimes in the order of 3 times those noted at the stirrup welds. However, these very large stresses did not occur in locations where fatigue cracks were likely to form.

Static Local Finite Element Analyses

The global analyses showed the bending moments, shear forces, and global deflections and deformations of the joints under a wide range of loadings. However, they did not provide a good indication of the true state of stress in the critical stirrup location. The center beam and the stirrup were modeled with a detailed local model, as depicted in Figure 10. The center beam was modeled with shell elements, and the stirrups were modeled with three-dimensional brick elements. The loads at the ends of the tube and the spring loads attributable to the elastomeric springs were obtained from the global computer analysis results. Note that the mesh used in this local analysis and shown in Figure 10 was appropriate for determining local stress and deformation, but the mesh was not fine enough to determine stress concentrations.

Local deformations had a considerable impact on the stirrup connection location. Figure 11 shows the typical local deformation obtained from one of these local analyses. The local analysis performed with gravity loads only showed considerable local bending deformation of the walls of the tube near the stirrup weld. The bending stresses caused by these plate bending moments were computed, and the stresses at the critical location were found to be approximately the same magnitude as the basic beam bending stress described earlier in the global analysis. These bending stresses varied from tension to compression through the thickness of the wall of the tube. However, these local bending stresses usually caused increasing stress (tensile) on the inside of the tube and decreasing stress on the outside of the tube near the stirrup weld in the absence of precompression in

the elastomeric springs. If the springs were precompressed, the local bending moments changed somewhat. This change in local bending moments could change the magnitude of the plate bending moment at some locations, and ultimately might cause tensile bending stress at the outside of the tube at the critical location.

Dynamic Analyses

Dynamic analyses were also performed. The basic dynamic analysis consisted of modal analysis with the global model described earlier. The mass of the components of the modular expansion joint were added to the model, and a large number of modes of vibration was computed. The damping of the system was unknown, and therefore, no damping was used in these analyses. However, note that damping must be relatively large (20 percent of critical or more) before significant changes in the dynamic periods are noted. The dynamic modal computations were slow because of the broad distribution of mass and stiffness and the large number of degrees of freedom. In most modal analysis, only a few modes of vibration need to be considered because the modes are well spaced and the largest part of the mass is participating in very few modes. However, the modes of vibration for this modular expansion joint were quite different. For example, the modes were closely spaced, and many hundreds would be needed to include the predominate portion of the mass in three-dimensional vibration. Nevertheless, the procedure produced some general observations that are worth noting.

First, the longest period modes were associated with horizontal movement. The majority of the participating mass (98+ percent) for the two translational degrees and one in-plane rotational degree of freedom were included in modes with periods of between 0.16 and 0.035 second. These translational degrees of freedom occurred because of deformation of the elastomeric springs. As noted earlier, the stiffness of these springs was not precisely known, but a 100 percent increase in stiffness would decrease the period by approximately 30 percent. A 50 percent decrease in elastomer stiffness would

increase the period by approximately 40 percent. These variations in elastomer stiffness are possible, but they represent upper limits on the probable variation.

The horizontal vibration required a large number of modes of vibration to include the total response, but the vertical gravity load response required many more modes of vibration. Figure 12 shows two typical vertical modes of vibration, which produced vertical response in the 13th center beam (CB13). The vertical modes of vibration with significant participating mass had periods ranging from 0.05 second to 0.005 second, and there were many, similarly closely spaced modes, each with a modest participating mass. Many modes were needed to completely describe the response of the 14 center beams and the support bars. However, the period of these vertical modes of vibration were about 0.015 second for the majority of the participating mass of the system.

In past inspections of the third Lake Washington Bridge joints, evaluators noted that the elastomeric bearings were sometimes loose and not precompressed. A lack of precompression reduces the stiffness of these bearings because they cannot act in tension without the precompression. As a result, several analyses were performed to evaluate the effect of loose bearings. The analysis indicated that an individual loose bearing might double the period of a single critical mode but would have minimal effect on most modes of vibration. An increased number of loose bearings might increase the period of a larger number of modes of vibration, but the relative magnitude of the period increase would often be smaller than that noted for a single mode.

Pattis and Tschemmernegg did not estimate the frequencies or periods for tubular center beams. [6] The periods estimated by Tschemmernegg for other modular joint systems were somewhat shorter than these finite element predictions. [1] The Tschemmernegg estimates appear to be based on rigid supports. The longer periods produced in the finite element analyses were largely caused by the elastomeric springs.

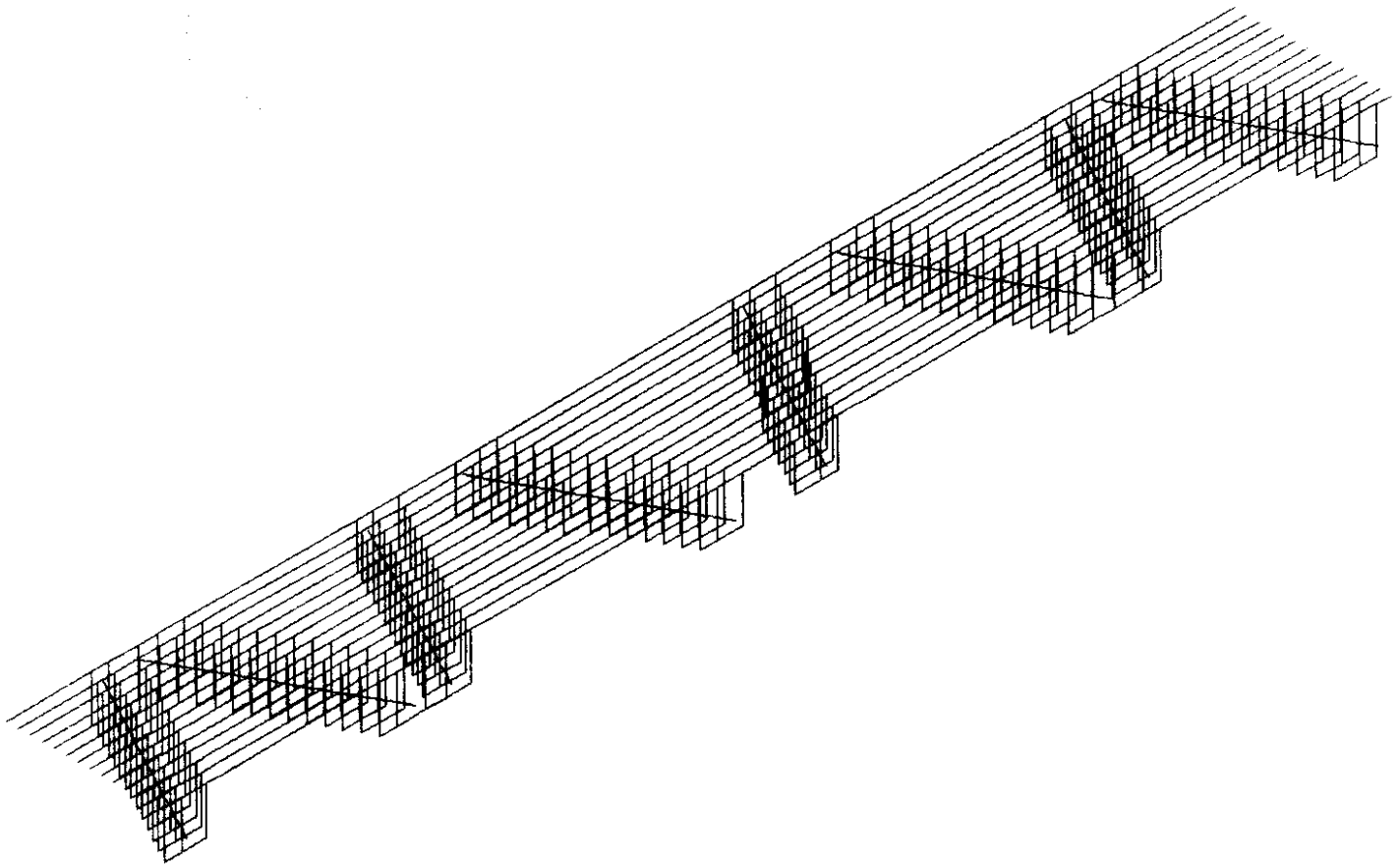


Figure 5. Finite Element Model of Entire Modular Expansion Joint
LM Line Pontoon A1 or R1 Eastbound



Figure 6. Model of Typical Center Beam

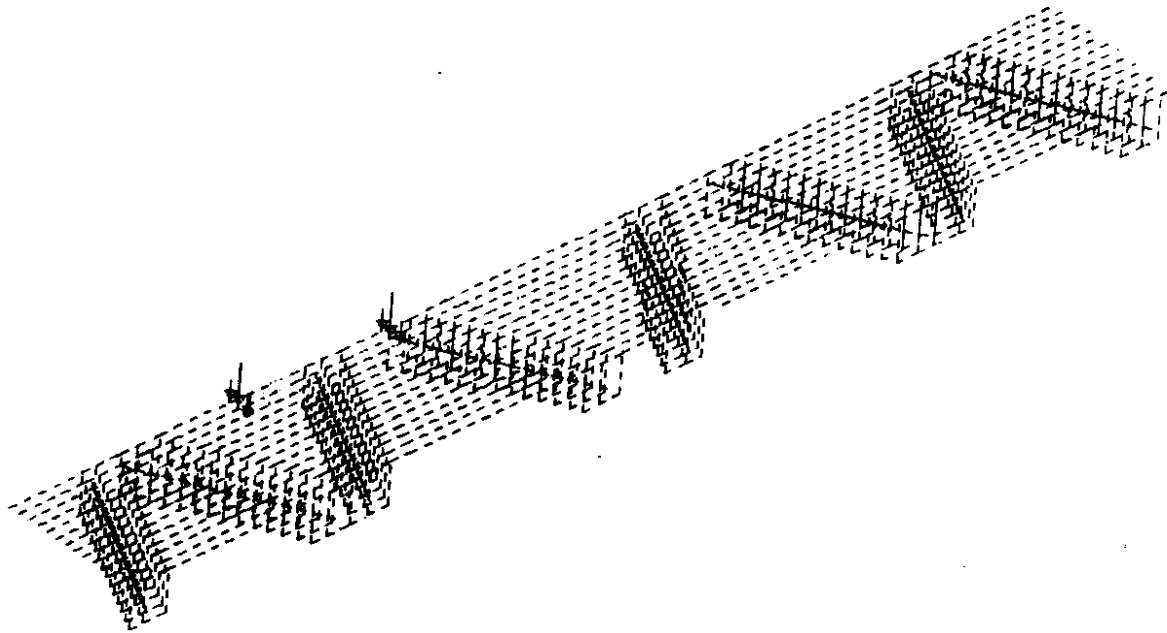


Figure 7. Typical Load Placement on Modular Expansion Joint
LM Line Pontoon A1 or R1 Eastbound

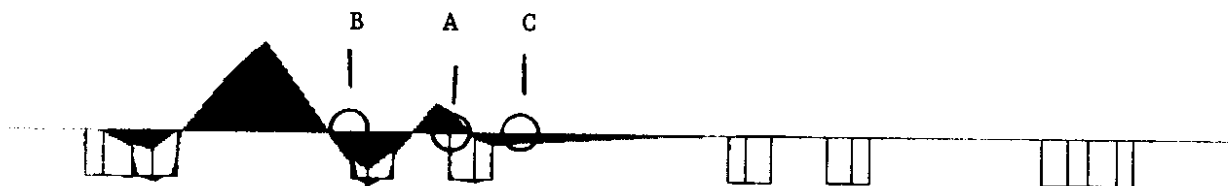


Figure 8. Bending Moment Diagram for a Center Beam at the Edge
of the Joint and with Truck Wheels in the Outside Lane

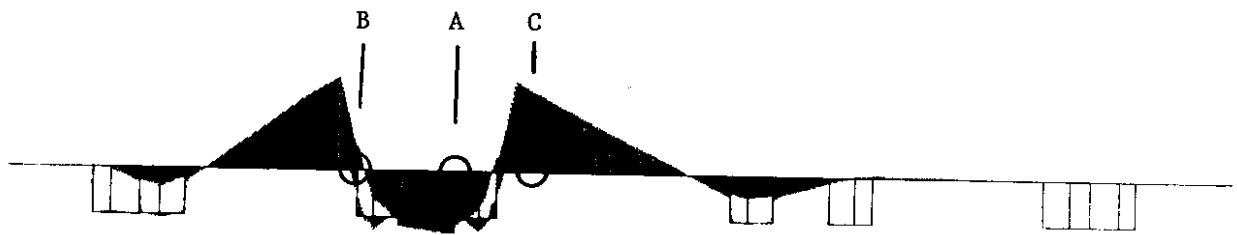


Figure 9. Moment Diagram for the Center Beam of Figure 8 with Wheel Loads in the Adjacent Lane of Traffic

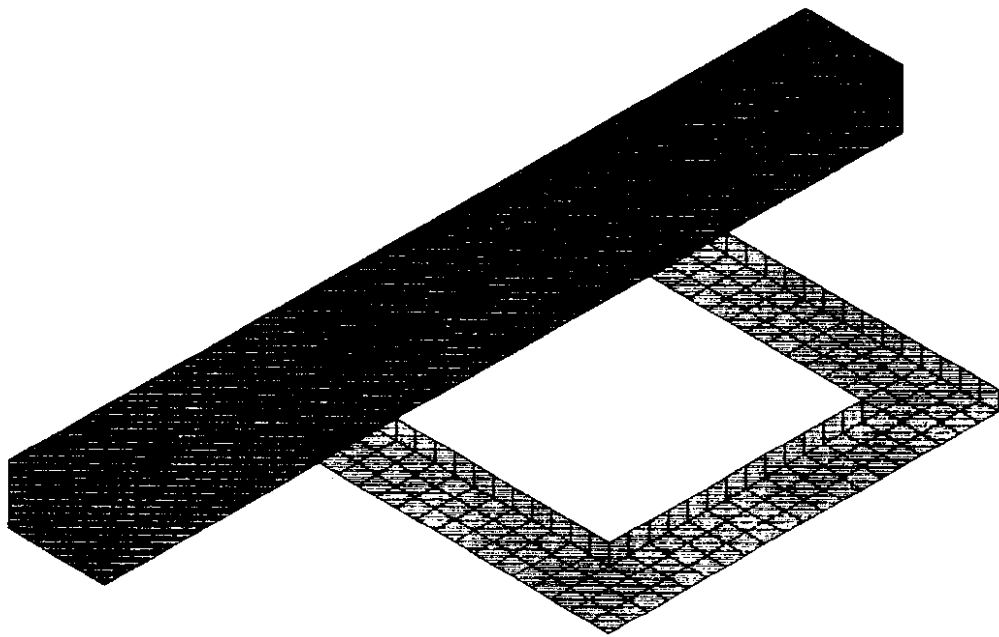


Figure 10. Local Finite Element Model

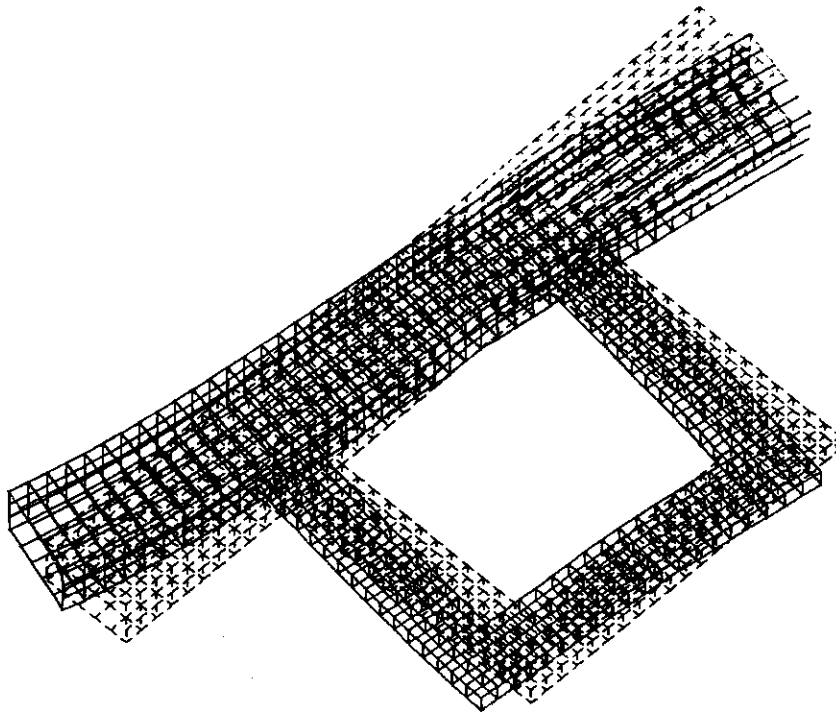


Figure 11. Local Deformation of the Stirrup and Center Beam

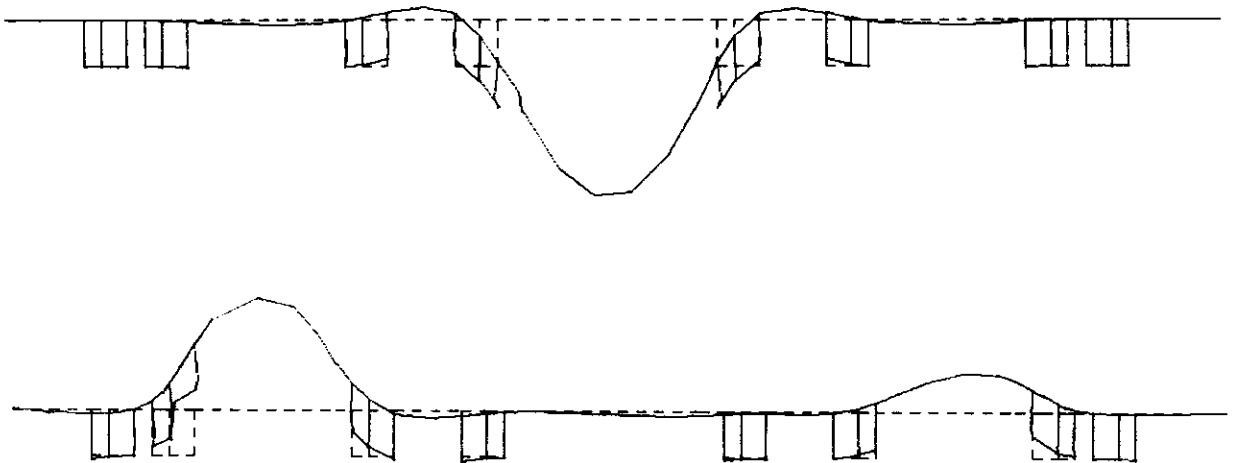


Figure 12. Typical Vertical Modes of Vibration

DISCUSSION

COMBINATION OF STATIC AND DYNAMIC RESPONSE

The prior discussion described the results of global and local analyses under static load and modal analysis of the global system. Stresses and stress ranges were computed for gravity and horizontal loads, and these stresses are useful in assessing the fatigue potential of the joint. However, the prior calculations did not include impact, and impact is commonly included in fatigue design.

Impact represents the dynamic amplification of the system attributable to the dynamic loading. The loading is assumed to be distributed between three center beams according to the procedure of Tschemmernegg. The wheel load on any center beam is initially zero until the wheel makes contact with the given beam, and it reaches its maximum value when the wheel is centered over the given center beam. The load on a beam then decreases until the wheel separates from the beam. If the truck is traveling at a constant velocity, this translates into the linear time dependent load function shown in Figure 13. The duration of loading, t_d , depends on the truck velocity and a distance equal to 2 times the center beam spacing. With the spacing used for the DS1200 joints described in this study, vehicles at 20, 40, and 60, mph would have had durations of 0.042, 0.021, and 0.014 second, respectively.

Figure 14 shows the dynamic amplification [13] of a linear elastic system with this ramp function loading. The plot shows the dynamic response divided by the static response as a function of the ratio of the duration of the ramp loading to the period of the system. Note that a dynamic amplification of 1.0 implies that the structure feels the full static loading, and a factor greater than 1.0 implies impact or dynamic amplification. The figure shows that the structure feels the full static load and potential impact if the duration of the loading is longer than approximately 30 percent of the dynamic period of the structure. If the duration is less than 10 percent of the period, less than 30 percent of the

static load is felt by the structure. The maximum duration is approximately 0.042 at a 20-mph truck speed, and this duration is similar to the shortest dynamic periods associated with horizontal movement and deformation. The duration at 60 mph is 0.014 second, and this is less than 50 percent of the shortest periods associated with significant horizontal movement. This suggests that significant amplification of horizontal forces should be expected at slower vehicle speeds. High speed vehicles may cause the expansion joint to experience the static force or slight attenuation. Thus, the expansion joint may not experience the large lateral loads suggested by the Tschemmerneegg method. It should be emphasized that this observation is meaningful only for this particular modular expansion joint system because of the transverse flexibility of the joint. Other modular joints (particularly multiple support bar systems) may be much stiffer and feel this full loading and possible dynamic amplification.

The dynamic periods for vertical movement and deformation are in the range of 0.052 to 0.005 second. The duration of loading varies between 0.015 and 0.042 second with truck speeds between 60 and 20 mph, respectively, and Figure 12 suggests that the joint will experience the full static load plus significant impact, because the ratio of the duration to the period is approaching 1. Note that these analyses neglect the effect of the vibration of the suspension system of the truck and additional impact caused by the uneven riding surface of the roadway and the joint. Thus, somewhat more amplification is possible in Figure 12 when these additional factors are considered, but the maximum amplification will always occur when the duration of loading, t_d , is similar to the periods of the center beam and the truck suspension system. It is also useful to note that the periods computed by Tschemmerneegg for vertical vibration are shorter than those computed for this modular joint. Short periods lead to large $\frac{t_d}{T}$ ratios, and Figure 14 shows that less amplification is expected under these conditions. Thus, these computer analyses suggest that gravity loads may be amplified more than suggested by

Tschemmernegg, but the maximum horizontal loads may be amplified less than suggested by the Tschemmernegg method.

HORIZONTAL COMPONENT OF FORCE

The horizontal component of force expected during traffic loading was also considered. This horizontal force is the basic time-dependent horizontal forcing function shown in Figure 11, which could be amplified (or reduced) by dynamic response. The expansion joint is sloped because of bridge geometry and changing lake levels, and gravity loading contributes a horizontal component of force to the joint because of this sloped condition. The shop drawings suggested that this slope varies between 2.3 percent and 4.0 percent. Because of this geometric effect, the horizontal component of force on the joint would be in the range of 2 to 4 percent when vehicles were uniformly braking or accelerating to maintain a constant speed. Larger horizontal components of force are possible when vehicles are braking to reduce their speed or accelerating to increase their speed. The observations regarding dynamic amplification still apply, and the horizontal force should be amplified most with slower traffic, while severe acceleration and braking forces are less probable with slower vehicle speeds. As a result, a 20 percent horizontal load may be conservative for this modular joint system. Field measurements would be helpful to support (or refute) this observation.

CORRELATION OF COMPUTED STRESS TO FATIGUE CRITERIA

Efforts were made to correlate the computed stress ranges with existing fatigue criteria. Static analysis has shown that the computed stress levels at the critical stirrup location may be large. Note that the stresses were computed from basic beam bending behavior for gravity and lateral loads. The stresses computed at the critical stirrup location (Location A on CB 13, as illustrated in Figures 8 and 9) are tabulated in Table 1. This location was selected because it produced both large tensile and large compressive stresses, and it was a typical location for a number of the cracks observed on the subject

joints. More than 60 percent of the visible cracks observed during an inspection of the four DS1200 joints in January 1993 were in similar locations. Larger stresses were noted at several other weld locations, and these typical values are tabulated in Table 2. Table 2 also contains maximum stress values for stirrup weld locations on other center beams, but Table 2 contains less complete calculations for considering impact, horizontal load, local bending effects, and variability in geometry and loading than shown in Table 1 for critical location A.

Normal AASHTO fatigue design is based on 2 million repetitions of the HS-20 truck loading. The stress range is the difference between the maximum loaded stress with impact and the unloaded condition. The welded stirrup-to-center beam detail is somewhat analogous to AASHTO's fatigue detail 17 because an external element (the stirrup) is welded to the beam flange. Detail 17 indicates fatigue category D or E, and these categories are illustrated in Figure 15. Category D requires a maximum stress of 7 ksi (48.3 MPa) if more than 2 million cycles are employed, and no more than 4.5 ksi (31.1 MPa) are permitted for Category E. Further, 2 million truck passes will cause far more than 2 million cycles of wheel loading, and so this limit should be applicable. Table 1 shows a maximum stress of -3.9 ksi (in compression) (-26.9 MPa) without dynamic amplification for LP3. When local bending effects are added, the maximum stress is 6.6 ksi (45.5 MPa). When dynamic amplification is added, it is clear that the stress exceeds the fatigue limit for either Category D or E conditions. The addition of horizontal load further aggravates this problem. Note, however, that the existing joint has not experienced 2 million cycles of HS-20 wheel loading in the short time it has been in service. This suggests that the detail is closer to the more critical Category E condition, the wheel load is larger than 16 kips (71.2 kN), or there is more dynamic amplification than suggested by the Tschemmerneegg method. Figure 14 clearly indicates that greater amplification is possible, particularly when the suspension system of the truck is considered. Further, the dynamic response associated with Figure 14 would result in

stress reversals on unloading, which could increase the stress range over that used by the simple AASHTO method.

Table 1 also shows that very different stresses occur at the critical stirrup location when the truck axle passes over a different line of travel (LP3 as opposed to LP2). Complete stress reversals are possible when the cyclic stress is caused by these alternate truck path loadings, and Table 1 indicates that a stress range of 6.6 ksi (45.5 MPa) without local bending and 13.0 ksi (89.7 MPa) with local bending should be expected with a 16-kip (71.2-kN) wheel load without horizontal load or impact. If 30 percent impact is added to this stress range, the range becomes 8.6 ksi to 16.9 ksi (59.3 to 116.6 MPa). Dynamic amplification clearly raises the stress range to a level well above the fatigue limit for AASHTO Categories D and E. Further, the analyses were performed with the modular joint in its intermediate opened position. If the joint is opened to its maximum width, a larger portion of the load is carried by the most heavily loaded center beam. Table 1 suggests that this maximum opening will result in stress ranges that are 30 percent larger than those noted above. An HS25 loading with 30 percent impact, a maximum opening, but no horizontal load would result in a 13.9-ksi (95.9-MPa) stress range without local bending effects and 27.4 ksi (189.0 MPa) with local bending effects. AASHTO category D suggests approximately 100,000 cycles, and category E suggests approximately 30,000 cycles for this condition when local bending is considered with this HS25 loading and impact. It should be emphasized that the stress state considered in AASHTO fatigue detail 17 does not consider local bending effects, and the above estimates should be viewed with caution. However, the local bending effect likely plays a role in the fatigue cracking. Further, category D would still predict only several hundred thousand cycles if the local bending effect were neglected. It should be emphasized that these ranges do not include any horizontal load. In addition, the stress range used in this evaluation requires passage of two trucks. The trucks do not pass simultaneously, but they pass over the joint in different travel paths. It is reasonable to

expect one cycle of this higher stress range with each truck passage, but clearly this passage would be very damaging. Further, smaller amplitude cycles can be expected with each wheel passing over the joint, and this accumulated damage would further reduce the number of cycles of severe loading that the joint could sustain.

The proposed AASHTO LRFD specification [14] utilizes a somewhat different fatigue evaluation procedure, and it may be useful to compare the observed stress levels to this proposed procedure. The LRFD provisions use fatigue categories and details similar to those used in the existing AASHTO provisions, and so detail 17 and category D or E again appear to approximate the stirrup-to-center beam weld detail. Figure 17 shows the proposed S-N curves for the LRFD categories D and E. The LRFD procedure and the existing AASHTO procedure are similar, except that LRFD recognizes that a single truck passing may cause more than one cycle of loading. However, the number of cycles is still limited to a maximum of two cycles per truck, and the definitions do not seem to be fully appropriate for a modular joint system. The S-N curves of the LRFD procedure are a straight line in the log-log plot for all stress ranges. There is a constant amplitude fatigue limit, but the curves suggest that even small cycles of stress may accumulate fatigue damage if the constant amplitude fatigue limit is exceeded by even a few cycles of stress. In view of these factors, the LRFD provisions may suggest a slightly shorter fatigue life than the AASHTO procedure, but the overall results should not be dramatically different. However, if a complete and accurate spectrum of stress ranges were available, the LRFD S-N curves could lead to a significant reduction of fatigue life if combined with a damage accumulation model.

Tschemmerneegg and Pattis [6] conducted one fatigue test on a tubular center-beam-with-stirrup detail, such as those used in the third Lake Washington Bridge. Figure 3 shows the S-N curve generated from this single test result. Using the proposed Tschemmerneegg fatigue design loads, they suggested that the fatigue life would be 10 million cycles of total truck loading. It should be emphasized that this estimate is

different from the AASHTO and AASHTO LRFD [14] life estimates in that it includes the total number of truck passings and an estimate of accumulated damage. The accumulated damage estimate is based on wheel load frequencies proposed for expansion joints in Europe. Fatigue cracks were noted approximately 18 months after the bridge was opened to traffic, and 10 million cycles would require approximately 18,000 axles for one lane of traffic per day. A traffic count performed in 1990 found that the westbound lanes of the bridge experienced approximately 6,720 axles of bus and truck traffic during the busiest 12-hour period of a normal work day. When the traffic was distributed over three lanes and the lighter weekend traffic was considered, the accumulated traffic was less than 20 percent of that suggested by the fatigue life estimate. [6] Further, the cracks obtained in the fatigue test were quite different than those obtained on the third Lake Washington Bridge. [6] Figure 16 shows the fatigue cracks developed in the Tschemmerneegg and Pattis test specimen. The initial and predominant cracking was longitudinal cracking along the edge of the stirrup-to-center beam weld. This cracking is different than the transverse-through-depth cracking seen on the Lake Washington Bridge and illustrated in Figures 1 and 2. No longitudinal cracking has been noted on the third Lake Washington Bridge, and there has been no evidence that such cracks are forming. Transverse cracking was eventually noted on test specimen, but it occurred only after the longitudinal crack had grown large and it did not progress through depth of the center beam. [6] This observation demonstrates that the Tschemmerneegg method produces a different mode of fatigue failure than that observed in the third Lake Washington modular joint. It further indicates that the Tschemmerneegg procedure may not be applicable for all joints and conditions.

While the Tschemmerneegg method does not replicate the fatigue problem noted in the Third Lake Washington Bridge, the stress ranges predicted by the test may not be unrealistic. The reason for the approximate accuracy of the S-N curve is that the modular joint details are likely to always be close to AASHTO categories D or E because the weld

detail is similar to AASHTO fatigue detail 17. The detail may be closer to category D if the modular joint is less susceptible to fatigue and closer to E if it is more susceptible. The log-log plot commonly used for S-N curves further masks the differences between more fatigue sensitive and less fatigue sensitive joints. This is illustrated in Figure 17, where a typical S-N curve range of different modular joint systems proposed by Tschemmerneegg and Pattis are compared to the S-N curves for AASHTO LRFD categories D and E. [14] The figure shows that all curves have a similar range of constant amplitude fatigue limit, but the AASHTO curves permit smaller stress ranges for higher stress levels and smaller numbers of cycles. Part of this difference can be attributed to the approximate load history commonly used in the U.S. and the procedures used to model accumulated damage in European practice.

The Tschemmerneegg procedure may not be applicable to elastically supported single support bar systems such as the swivel joist system. These systems may be more susceptible to amplification of the gravity loads (i.e., dynamic impact) because of its stiffness characteristics. Further, the static analysis shows larger stress ranges than those suggested by the Tschemmerneegg method because of variation in the travel track of the truck across the modular joint and the geometry of the joint. Nearly complete stress reversals are possible because of these load variations, while Tschemmerneegg uses only a 40 percent load reversal (uplift force). Finally, the Tschemmerneegg method is based on application of an accumulated damage model to a load spectrum based on data from three or four bridges in Europe. Truck loads vary considerably from state to state in the U.S., and there is evidence of overweight truck traffic. However, there is no indication of how wheel loads vary in the U.S. Agarwal performed a series of field measurements on a modular expansion joint on a bridge in Ontario, Canada, and his measurements suggested that the load range and spectrum were different than those used by Tschemmerneegg. [8] The combined effect of these observations make the fatigue behavior of modular joints more variable than suggested by the design method.

OTHER ISSUES

A number of issues are related to the fatigue behavior of modular joints.

Lake Level and Seasonal Effects

The level of the lake may have some impact on the fatigue of the center beams in this modular joint system. The lake level tends to lower during the early autumn and raise during the spring. It is normally at its lowest in early or mid-autumn. Lower lake levels increase the slope and opening of the modular expansion joint. The increased opening results in an increased load on the most heavily loaded center beam. This is illustrated in Table 1, which shows that opening the joint to its maximum increases the stresses and stress range approximately 30 percent over the figures obtained in the basic analysis.

Past analysis has suggested that horizontal loads are likely to be amplified more when the bridge traffic is moving slowly. Seattle rush hour traffic generally appears to be more congested during the late summer and fall, but it flows more rapidly in the late spring and early summer. Horizontal forces significantly increase the stress range in the center beams and decrease the fatigue life, but as noted previously, the horizontal force is likely to be amplified more by impact when the traffic is moving slowly. Further, the dynamic horizontal force is likely to be largest when the slope is greatest and the joint is at its widest configuration. All of these factors appear to converge in approximately October, and so it appears that the most adverse conditions for fatigue occur at that time. Table 1 illustrates the combination of a 16-kip (71.2-kN) HS-20 wheel load with 30 percent impact and 20 percent horizontal load. The 20 percent horizontal load was estimated to be a maximum rational force in a previous discussion. The maximum stress range, excluding local bending effects, is approximately 17.9 ksi (123.5 MPa), which, by the proposed Tschemmerneegg and Pattis S-N curve, suggests a maximum of approximately 800,000 cycles, or 100,000 to 600,000 cycles according to AASHTO

categories D and E. Local bending effects could double the stress range and further reduce the fatigue life.

This postulated worst case fatigue condition appears to be consistent with observed fatigue cracking, since WSDOT records suggest that most fatigue cracks were observed during this period or shortly after this critical period ended.

Effect of Tubular Center Beams

The tubular center beams may also affect the fatigue life of the modular joint system. Table 1 clearly shows that local bending deformation of the walls of the tube increased the maximum stress and stress range of the center beam. This local bending deformation contributed to the mode of failure observed in the Tschemmernegg test, but the deformation observed in the analysis (and suggested by the mode of failure in Figures 1, 2, and 16) is quite different from that noted in the test specimen. [6] The local bending deformation increased the maximum stresses and stress range by approximately 100 percent. It is difficult to estimate exactly how much the local bending shortened the fatigue life because the test result does not apply and the stress is quite different for the normal beam bending stress and the stress envisioned by the S-N curves for AASHTO categories D and E. While the local bending deformation of the tube reduced the fatigue life of the third Lake Washington modular joint system, it was not the only cause. The large stresses and stress range of the global analysis without local bending indicated that fatigue cracking would still have occurred even if the local deformation had not been present.

Residual Stress

Residual stresses in the tube also influenced the fatigue life of these tubular center beams. Residual stresses are introduced by all fabrication processes. The formation processes for the steel tubes, the welding processes required to connect the stirrup and cover plates to the center beams, and the welding required to splice the tubes and their infill stiffeners all introduce residual stress. However, the welding of the stirrup to the

center beam is the final process in the critical cracking area, so its residual stresses have the greatest effect on the fatigue of the center beams. Welding introduces a concentration of heat in a limited area. The heated area cools relatively quickly after the welding is complete because the heat is conducted to the surrounding, unheated metal. The heat affected zone of the weld experiences thermal shortening as the cooling occurs. The shortening is resisted by the surrounding, unheated metal, and large tensile residual stresses develop. The tensile residual stress is often similar to the yield stress. However, the residual stress is affected by the sequence of welding. Large welds, such as those required to attach the stirrup to the center beam, usually require multiple passes, and later passes may reduce the tensile residual stresses at the earlier welded locations. This makes the actual magnitude and distribution of the residual stress around the stirrup weld uncertain. However, there is reasonable certainty that the residual stress near the weld is a large tensile stress.

The tensile residual stress may influence the fatigue of the center beams. The computer analysis showed that many of the cyclic stresses induced by wheel loading were compressive stresses. These compressive stresses cause concern because cyclic compressive stresses are not normally considered to be a source of fatigue cracking. However, the compressive stresses are added to the existing residual stress, and as a result the entire stress range may be in tension. Thus, the tensile residual stress may affect the fatigue cracking significantly. The actual effect is impossible to quantify because the magnitude and distribution of the stress at the critical crack location are uncertain.

Fatigue Cracking in Other Center Beams

The previously described analysis focused on location A of center beam CB13. Other stirrup locations, such as B and C (see Figures 8 and 9), experienced larger stresses, and some of these global stress ranges are noted in Table 2. These are also clearly fatigue sensitive locations, as can be seen by comparing these stress ranges to the S-N curves from earlier discussion. Critical location B (see Figures 8 and 9) was at a stirrup weld.

However, it was on the inside of a longer span, and approximately 25 percent of the fatigue cracks on the bridge's joints were noted in similar regions. Critical location C was at the end of a center beam flange cover plate, and one fatigue crack was found at this location. Note that this location is more similar to AASHTO fatigue detail 7, and a somewhat different S-N curve may be expected. However, the analysis performed at these other locations was not as extensive as that performed for location A, for the reasons noted earlier. However, examination of these results clearly indicates a considerable fatigue potential at numerous locations on the center beams near the edge of the DS1200 joint. The potential is present because large stress and stress ranges are caused by the variable span lengths of these edge beams.

Middle center beams have more uniform span lengths, and as a result the maximum bending stresses at the stirrups are significantly smaller. This is also illustrated by the stress range for a middle center beam (CB7) in Table 2. Figures 18 and 19 illustrate the moment diagram of load positions LP2 and LP3 of CB7. The stirrup-center beam joint labeled joint D in these figures appears to experience the largest stress reversal. The maximum bending stress at this critical location with a 16-kip (71.2-kN) static wheel load is -2.1 ksi in compression and 1.9 ksi in tension (-14.5 and 13.1 MPa). These maximum stresses and stress ranges are approximately 40 percent to 60 percent of the values noted for CB13. However, fatigue is still likely to occur at these center beams because heavier wheel loads, dynamic amplification (impact), horizontal loads, and residual stress will all combine to produce stresses that exceed the fatigue threshold. Nevertheless, the lower stress range will significantly delay the initiation of fatigue cracking.

While there is no accurate S-N curve for the center beams of this modular joint system, a rational procedure can be used to estimate their fatigue potential and possible fatigue life expectancy. Figure 20 illustrates the delay of fatigue cracking at these less stressed joints. The S-N curve for the modular expansion joint is not known because

there is no reliable evidence to simulate the fatigue cracking observed on the third Lake Washington Bridge. However, the slope of virtually all S-N curves is held at -0.33 in the log-log plot. This slope is used by AASHTO LRFD and it is also used by Tschemmerneegg and European practice, and it means that an order of magnitude reduction in the stress range results in 3 orders of magnitude increase in fatigue life. If the average traffic volume is assumed to be more or less uniform over the bridge life, the number of cycles is linearly related to time, and time can replace the number of cycles in the S-N curve, as illustrated in the figure. Then the extended fatigue life with a 50 percent reduction in stress range can be estimated, as shown in the figure. Initial cracking on the edge center beams was noted in approximately 1.5 years and extensive fatigue cracking was noted in approximately 2.5 years. A 40 percent to 50 percent reduction in stress range suggests that initial cracking in this area should take 5 to 8 times as long to occur as the cracks at the maximum stress range location. At present, there is no cracking in the middle center beams. Thus, cracking of the middle center beams should be expected after approximately 8 to 15 years, and extensive cracking in the middle center beams should be present within 15 to 20 years. Thus, the middle center beams appear much less susceptible to fatigue cracking. The intermediate center beams, such as CB4 and CB11, are between the edge beams and the middle beams, and stresses in the order of 75 percent or 85 percent of the edge beam stresses are estimated. This equates to a fatigue life of approximately 1.5 to 2.5 times the life of an edge beam such as CB13. Initial cracks in CB4 or CB11 would be expected about 2 to 5 years after the bridge was opened to traffic, and extensive cracking in these intermediate center beams is probable after 6 to 10 years. These predictions are generally consistent with field observations, since 75 percent of the cracking has been observed in edge beams equivalent to CB13 and CB14. Approximately 18 percent of the cracking has been noted in intermediate beams equivalent to CB 4 or CB11, and only 7 percent has occurred in center beams interior to CB4.

Effect of Smaller Joint Size

Four of the modular joints on the Lake Washington Bridge were smaller (DS480), single support bar modular systems. To date, no fatigue cracks have been positively identified on these smaller joint systems, although several potential crack locations have been noted. However, these smaller joints are very difficult to inspect. Therefore, it is rational to ask whether fatigue is likely to be a problem on the smaller joints. The rationale described for middle and intermediate center beams can also be applied to the smaller expansion joints.

The single support bar, modular expansion joints have variable span lengths near the edge of the joint and uniform span lengths near the middle center beams. This variable span length has been shown to be a critical element of the fatigue potential. A global static analysis of the smaller modular joint was performed with the 16-kip wheel loads centered on an edge center beam. Table 3 summarizes some of the moments noted at critical locations of the DS480 joint, and these can be compared to locations A and B of CB13 of the DS1200 joint. The stresses and stress ranges are similar to those noted for location A of CB13 of the DS1200 joint, and to approximately 80 percent of those noted at location B. Approximately 60 percent of the observed cracking occurred at locations comparable to A, and 25 percent occurred at locations comparable to location B, despite its larger stress level. The geometry of the smaller DS480 joint makes the maximum stress locations more comparable to location B than to location A. As a result, it is likely to produce the proper S-N curve. Significant cracking has been noted at location B after 3.5 years, and the 80 percent stress level suggests that comparable cracking should be noted on the smaller joint after 8 years.

Replacement Center Beams

Heavier replacement center beams have been proposed for the third Lake Washington modular joints. Figure 21 illustrates the geometry of these beams. The beams are relatively wide, and fewer beams can be used if the required movement

capacity will be maintained. As a result of the greater width and spacing, a larger portion of the load is carried by an individual center beam when the joint is in its intermediate configuration. Further, the variable span lengths are not changed by the center beam replacement. A static global analysis with the replacement center beams was performed. Table 3 shows the computed stresses for locations A and B of an edge center beam, and these stresses can be compared to the computed stresses for CB13 at the same locations shown in Tables 1 and 2. The stresses from the global analysis actually increased slightly at location A, and they are approximately 70 percent of those noted at location B with the tubular center beams. A local analysis was not performed, but the geometry of the replacement center beams suggests that the local deformation and stress would be greatly reduced. In view of these factors, the replacement center beam would be unlikely to prevent future fatigue problems with the DS1200 joint. It might eliminate the potential for fatigue in the smaller DS480 joint, and the fatigue cracking would take longer to develop than in the existing joint. It is difficult to predict the actual life of the replacement beams because of uncertainty regarding the effect of local deformation in comparison to the global stress level, and because of the probability that the location of the fatigue cracking may move. If location A remained the critical point, the extended fatigue life might be shorter than it would be if it moved to a location such as location B. The tests by Tschemmerneegg suggested that the cracking might move to a different location with respect to the stirrup, but it is not possible to address this issue without performing an additional local analysis.

Variations in Wheel Loads and Geometry

The basic analyses described in this report used a 16-kip (71.2-kN) wheel load. The load was applied as a transverse line load on the joint or a point load on an individual center beam. Analyses were performed with and without horizontal components, amplification caused by impact, and different load placement positions. These analyses provided a good basis for comparison of individual results, but they did not necessarily

reflect the true stress in the actual bridge joint. Actual wheel loads are distributed over the width of the tire, and WSDOT does not permit a 16-kip (71.2-kN) wheel load for normal traffic or special permit vehicles. [15] Normal static wheel loads permitted by WSDOT are limited to 10 kips (44.5 kN) per wheel and 600 lbs/inch (0.106 kN/mm) of tire width. Special service vehicles, such as some garbage trucks and articulated Metro buses, are allowed to have larger wheel loads. These vehicles have maximum rated wheel loads of about 13 kips (57.8 kN) per tandem wheel. A series of analyses were performed to evaluate the effect of these rated wheel loads and the distribution of the wheel load over the width of a tire.

The basic distributed load analysis was performed with a 16-kip (71.2-kN) wheel load so that the stresses and moments could be directly compared to previously computed results. Figure 22 shows the distribution pattern used for these calculations. The loads were distributed between adjacent center beams, as noted previously. Therefore, the total load applied to the joint and to individual center beams was the same as that used for the basic 16-kip (71.2-kN) wheel load analysis. The distributed load usually reduced the bending stresses beneath those noted with the concentrated wheel load. This is illustrated in Table 4, in which the bending stresses obtained in the global analyses with a 16-kip (71.2-kN) concentrated wheel load are compared to the stresses obtained for the distributed load on CB 13 at several critical locations. The maximum stress levels were usually reduced by 10 to 20 percent with the distributed loading. However, the stresses and stress ranges increased at a few other locations. Thus, the net effect on the total stress range was somewhat smaller than 10 to 20 percent. Further, the loads were centered at the same location as that used for the concentrated loads, and larger moments and stresses would be possible if the loads were shifted slightly. As a result of these observations, it appears that the stress values and stress ranges with distributed loads would be about 85 percent of those computed with concentrated loads.

The maximum legal wheel load in the state of Washington is approximately 10 kips (44.5 kN). The maximum special permit wheel load is 13 kips (57.89 kN). When the wheel load is reduced to 13 kips (57.9 kN), the stresses and moments computed in the global analyses are 81.2 percent of those computed with a 16-kip (71.2-kN) load. Thus, the combined effect of the distributed wheel load and 13-kip (57.9-kN) wheel limit reduces the bending moments and stress to approximately 70 percent of those noted with the 16-kip (71.2-kN) concentrated load. It must be emphasized that these reduced values do not include dynamic impact, opening of the joint configuration, or horizontal load, nor do they consider the possibility that vehicle wheels are above legal limits.

Table 1. Stress Range Levels for Location A of CB13

	Stress or Stress Range (ksi)	
	Global Analysis (ksi)	Local + Global (ksi)
16 kip at Load Point (LP) 2 16 kip at Load Point 3 Stress Range Between 2 and 3	2.7 -3.9 6.6	6.4 -6.6 13.0
16 kip Wheel Load @ LP 2w/max. opening 16 kip Wheel Load @ LP 3 w/max. opening Stress Range Between 2 and 3	3.5 -7.2 10.7	8.3 8.6 16.9
Load Point 2 with HS25 and 30% Impact Load Point 3 with HS25 and 30% Impact Stress Range with HS25 and 30% Impact	4.4 -6.3 10.7	10.4 -10.7 21.1
LP 2 for HS25 w/30% Impact and max. open. LP 3 for HS25 w/Impact and max. open. Stress Range Between 2 and 3	5.7 -8.2 13.9	13.5 -13.9 27.4
16 kip with 40% horizontal at LP 2 16 kip with 40% horizontal at LP 3 Stress Range Between 2 and 3 with 40%	6.7 -7.9 14.6	
16 kip gravity with 20% horizontal at LP2 16 kip gravity with 20% horizontal at LP3 Stress Range Between 2 and 3	4.7 -5.9 11.6	
16 kip grav. w/ 20% horiz. & 30% Impact at LP2 16 kip grav. w/ 20% horiz. & 30% Impact at LP3 Stress Range Between 2 and 3	6.1 -7.7 13.8	
16 kip w/ 20% H, 30% I, & Max. Open at LP2 16 kip w/ 20% H, 30% I, & Max. Open at LP3 Stress Range Between 2 and 3	7.9 -10.0 17.9	

- = compressive stress
+ = tensile stress

Table 2. Stress Range Levels for Other Center Beams and Locations

	Stress or Stress Range (ksi)	
	Global Analysis (ksi)	Local + Global (ksi)
STRESS AT LOCATION B OF CB13 16 kip at LP 4 16 kip at LP3 Stress Range Between LP2 and LP3	-1.9 6.2 8.1	Not Avail. Not Avail. Not Avail.
STRESS AT LOCATION C OF CB13 16 kip at LP3 16 kip at LP4 Stress Range Between LP3 and LP4	1.6 -6.4 8.0	Not Avail. Not Avail. Not Avail.
STRESS AT LOCATION D OF CB7 16 kip at LP 2 16 kip at LP3 Stress Range Between LP2 and LP3	-2.1 1.9 4.0	Not Avail. Not Avail. Not Avail.

Table 3. Stress Range Levels for Other Joint Systems

	Stress or Stress Range (ksi)	
	Global Analysis (ksi)	Local + Global (ksi)
CRITICAL STRESS LOCATION FOR EDGE CENTER BEAM OF DS480 JOINT 16 kip at LP 1 16 kip at LP2 Stress Range Between LP2 and LP3	-3.9 1.0 4.9	Not Avail. Not Avail. Not Avail.
CRITICAL STRESS LOCATION FOR EDGE CENTER BEAM OF DS480 JOINT 16 kip at LP 1 16 kip at LP2 Stress Range Between LP2 and LP3	3.4 -3.3 6.7	Not Avail. Not Avail. Not Avail.
CRITICAL STRESS LOCATION FOR EDGE CENTER BEAM OF DS480 JOINT 16 kip at LP 3 16 kip at LP4 Stress Range Between LP2 and LP3	3.5 -3.2 6.7	Not Avail. Not Avail. Not Avail.
STRESS AT LOCATION A OF EDGE CB WITH REPLACEMENT BEAMS 16 kip at LP 2 16 kip at LP3 Stress Range Between LP2 and LP3	-2.5 4.3 6.9	Not Avail. Not Avail. Not Avail.
STRESS AT LOCATION B OF EDGE CB WITH REPLACEMENT BEAMS 16 kip at LP 2 16 kip at LP3 Stress Range Between LP2 and LP3	5.4 -1.3 6.7	Not Avail. Not Avail. Not Avail.

Table 4. Stresses for Concentrated and Distributed Wheel Loads on CB13

	Stress or Stress Range (ksi)	
	Global Analysis (ksi)	Local + Global (ksi)
	Concentrated Load	Distributed Load
STRESS AT LOCATION A OF CB13		
16 kip at Load Point (LP) 2	2.7	2.4
16 kip at Load Point 3	-3.9	-2.1
Stress Range Between 2 and 3	6.6	4.5
STRESS AT LOCATION B OF CB13		
16 kip at LP 4	-1.9	-1.5
16 kip at LP3	6.2	5.2
Stress Range Between LP2 and LP3	8.1	7.7
STRESS AT LOCATION C OF CB13		
16 kip at LP3	1.6	0.4
16 kip at LP4	-6.4	-5.9
Stress Range Between LP3 and LP4	8.0	6.3
STRESS AT OTHER LOCATIONS OF CB13		
16 kip at LP 3	1.5	0.4
16 kip at LP4	-6.4	-5.9
Stress Range Between LP2 and LP3	7.9	6.3

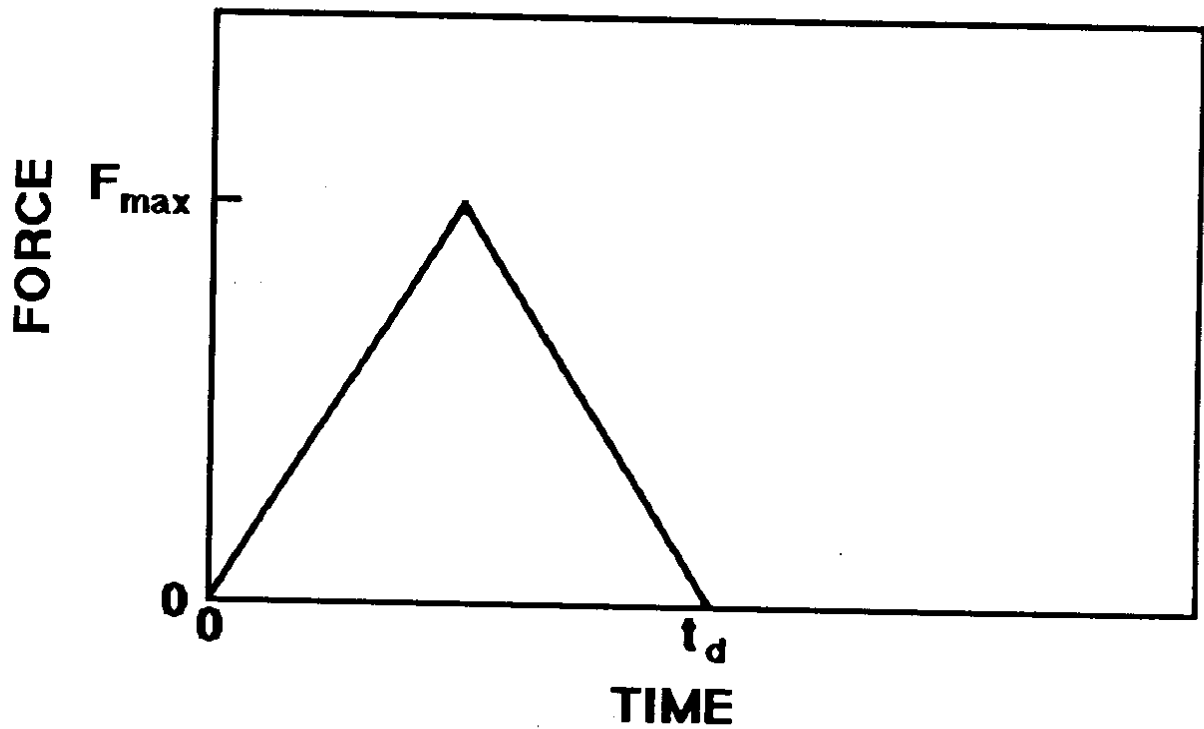


Figure 13. Idealized Dynamic Loading on a Center Beam

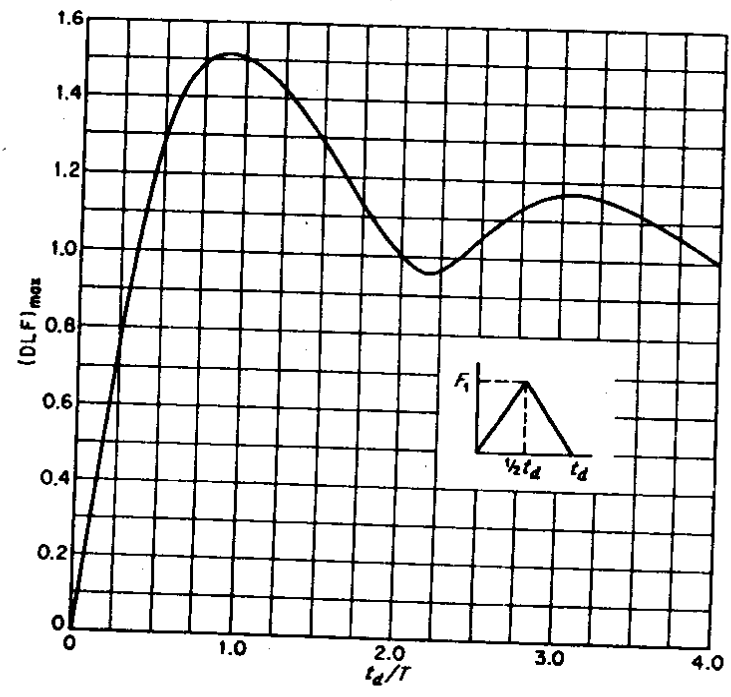


Figure 14. Dynamic Amplification for a Ramp Function Loading

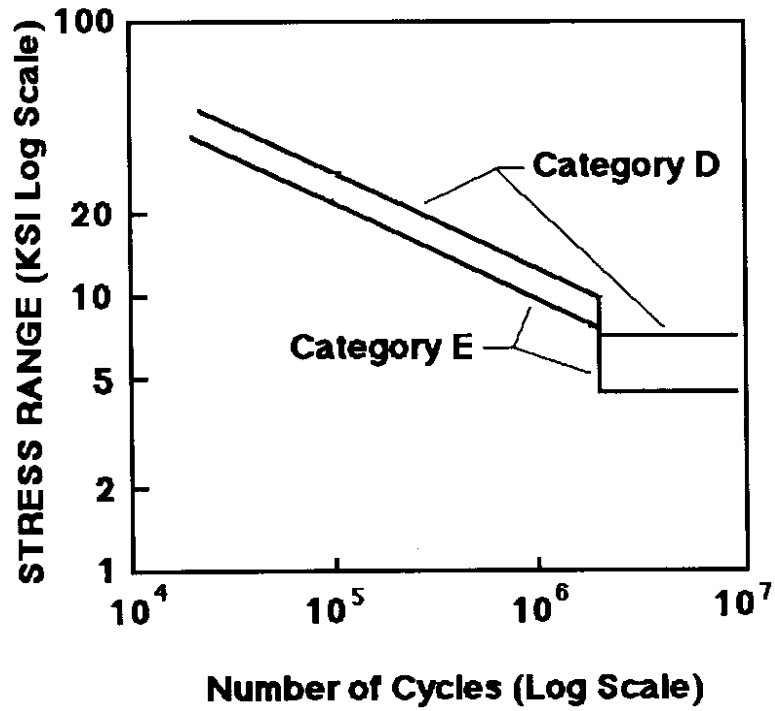


Figure 15. Present AASHTO S-N Curves for Categories D and E

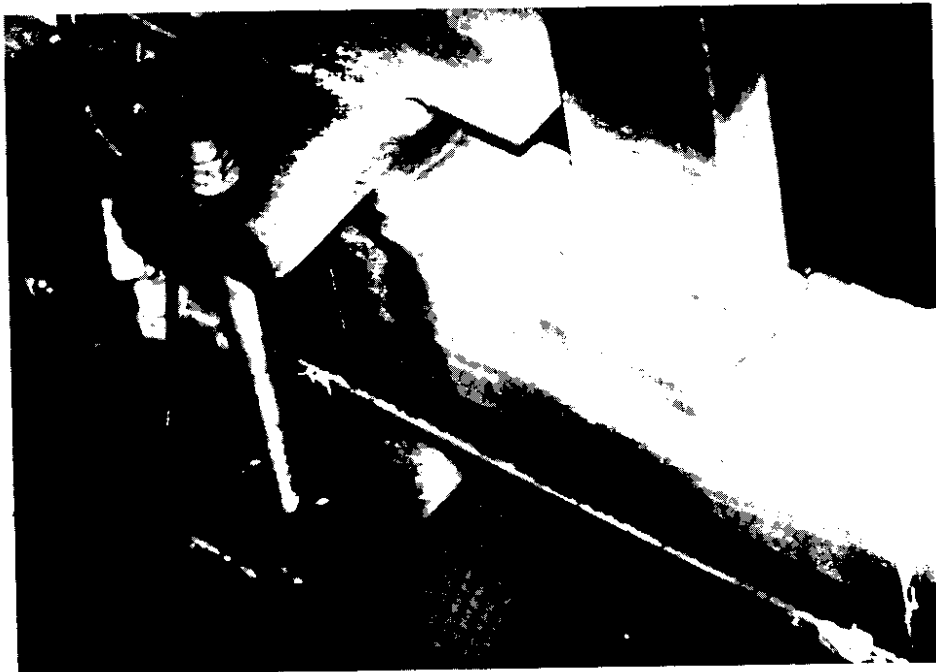


Figure 16. Photo of Fatigue Cracking from Tschemmerneegg Fatigue Test

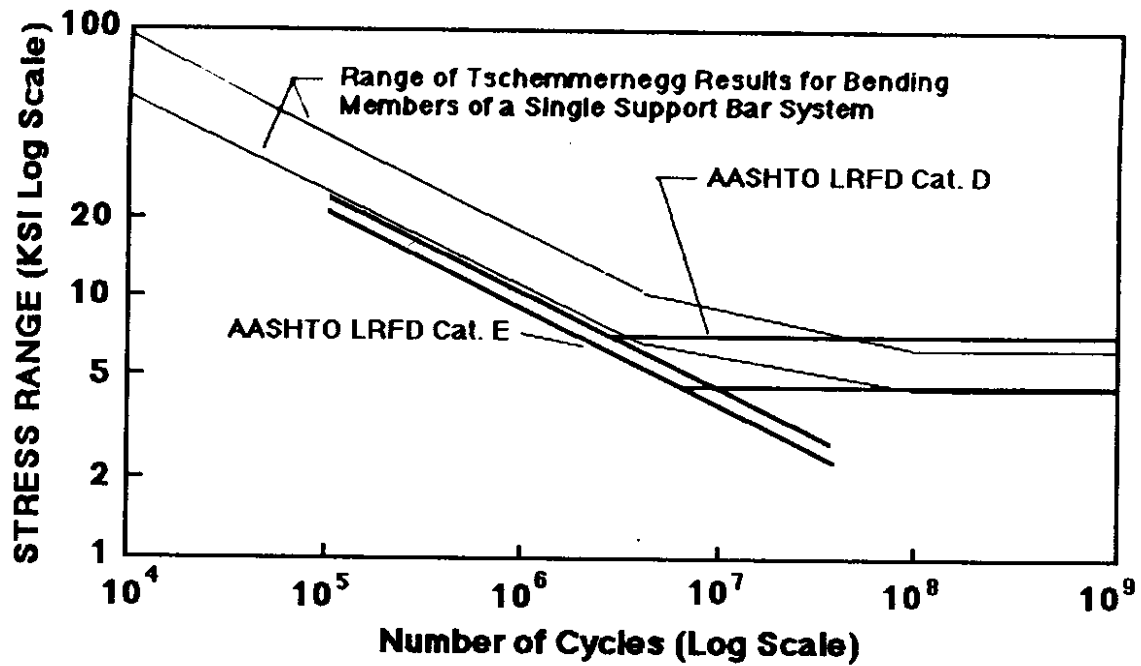


Figure 17. AASHTO LRFD S-N Curves Compared to a Range of Different Tschemmerneegg S-N Curves

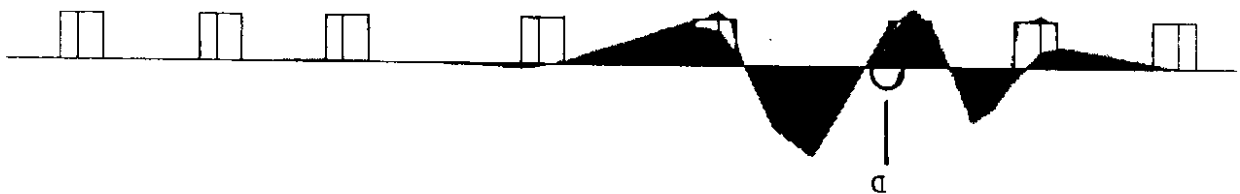


Figure 18. Bending Moment Diagram for a Middle Center Beam CB7 with Truck Wheels in the Outside Lane (LP 2)



Figure 19. Moment Diagram for CB7 with Wheel Loads in the Adjacent Lane of Traffic (LP3)

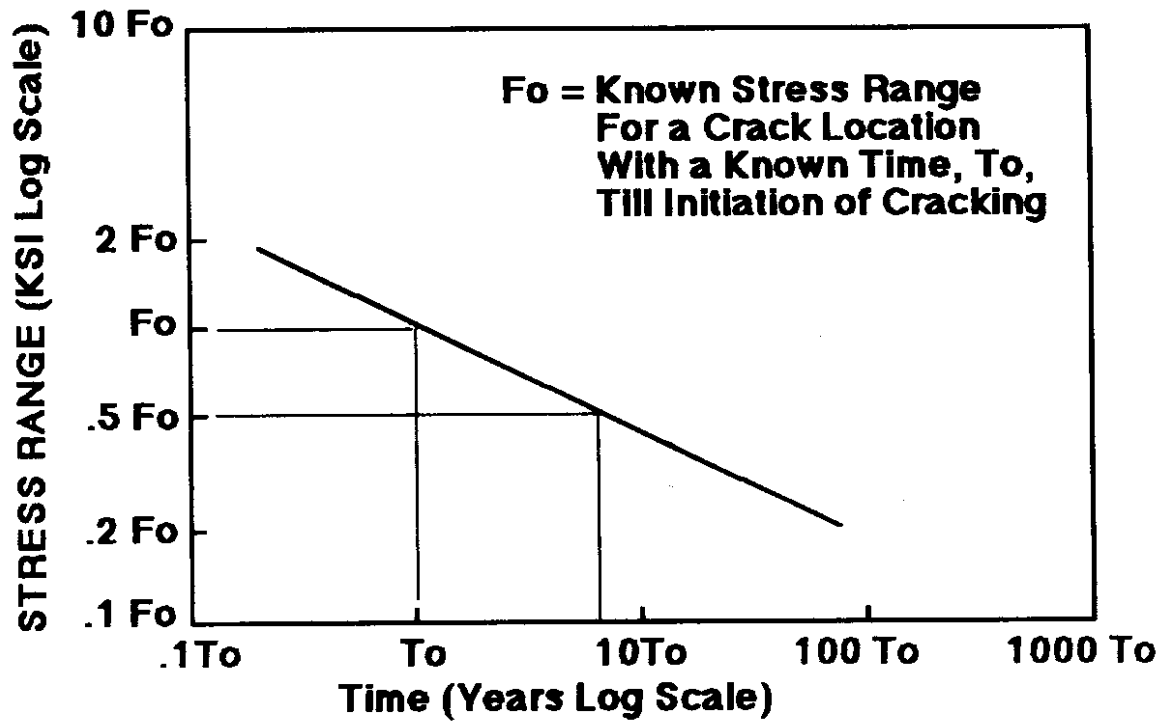


Figure 20. Approximate S-N Curve Translated to a Time Scale

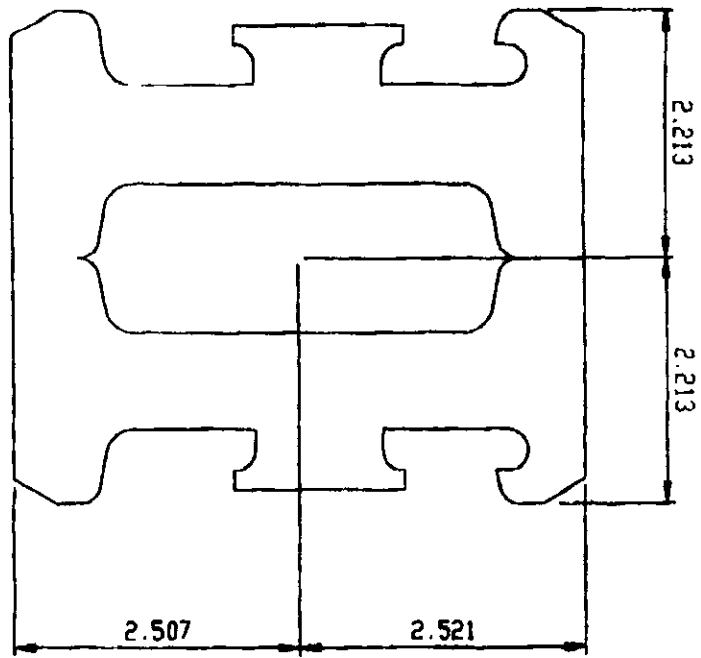


Figure 21. Geometry of Proposed Replacement Center Beams

Load is uniformly distributed over the width of two tires and distributed to center beams by normal method.

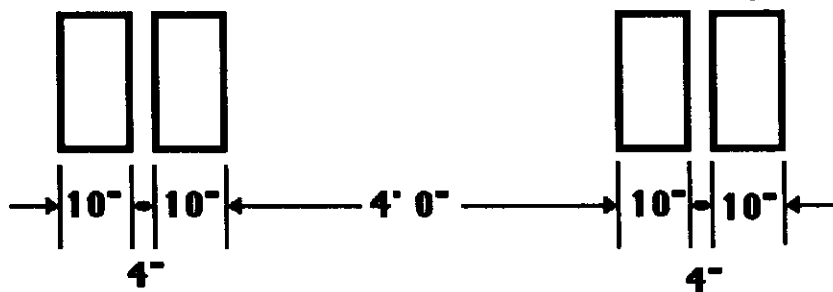


Figure 22. Geometry Used for Distributed Wheel Load

REFERENCES

1. Pattis, A., and Tschemmerneegg, F., "Fatigue Testing and Design of Modular Expansion Joints," Report Published by University of Innsbruck and The D.S. Brown Company, Innsbruck, Austria, March 1992.
2. Tschemmerneegg, F., "The Design of Modular Expansion Joints," Proceedings, 3rd World Congress on Joint Sealing and Bearing Systems, Vol. 2, Toronto, Ontario, Canada, October 1991.
3. "Fatigue Design and Testing For Expansion Joints," D.S. Brown Technology Bulletin No. 1, North Baltimore, Ohio, October, 1991.
4. Tschemmerneegg, F., and Pattis, A., "Measurements on Semi-Rigid Modular Expansion Joints on Nettetal-Bridge on Highway BAB 61 in Germany," Innsbruck, 15 March 1991.
5. Frost, N.E., Marsh, K.J., and Pook, L.P., Metal Fatigue, Oxford University Press, 1974.
6. Pattis, A., and Tschemmerneegg, F., "Fatigue Testing and Design of Modular Expansion Joints — The Brown/Maurer SWIVEL JOIST System — Repair Proposals for 3rd Lake Washington Bridge," Short Version of an Unpublished Report, August 1992.
7. Koster, Waldemar, "The Principle of Elasticity for Expansion Joints," ACI Publication SP-94, Joint Sealing and Bearing Systems for Concrete Structures, Volume 2, Detroit, Michigan, 1986.
8. Agarwal, A.C., "Static and Dynamic Testing of a Modular Expansion Joint in the Burlington Skyway", ACI, Third World Congress on Joint Sealing and Bearing Systems, Toronto, Canada, October 1991.
9. Roeder, C.W., "Preliminary Report on Fatigue Cracking in Modular Expansion Joints," Unpublished Report submitted to WSDOT, August 15, 1992.
10. Wilson, E.L., and Habibullah, A., "SAP90 — A Series of Computer Programs for the Static and Dynamic Analysis of Structures," Users Manual, Computers and Structures, Inc., 1918 University Ave., Berkeley, California, July 1989.
11. Stanton, J.F. and Roeder, C.W., "Elastomeric Bearings — Design, Construction and Materials," NCHRP Report 248, Washington, DC, September, 1982.
12. "Standard Specifications for Highway Bridges," 14th Ed., AASHTO, Washington, D.C., 1989.
13. Biggs, J.M., "Introduction to Structural Dynamics", McGraw Hill, New York, New York, 1964.

14. **"Proposed LRFD Standard Specifications for Highway Bridges," April 17, 1982 Draft, NCHRP 12-33, Washington, DC, 1992.**
15. **"Overweight/Oversize Vehicle Permits," WSDOT, Motor Carrier Services Office, Olympia, Washington, September 1990.**